THE IIOAB JOURNAL

VOLUME 3 : NO 1 : MAY 2012 : ISSN 0976-3104

Institute of Integrative Omics and Applied Biotechnology Journal

Dear Esteemed Readers, Authors, and Colleagues,

I hope this letter finds you in good health and high spirits. It is my distinct pleasure to address you as the Editor-in-Chief of Integrative Omics and Applied Biotechnology (IIOAB) Journal, a multidisciplinary scientific journal that has always placed a profound emphasis on nurturing the involvement of young scientists and championing the significance of an interdisciplinary approach.

At Integrative Omics and Applied Biotechnology (IIOAB) Journal, we firmly believe in the transformative power of science and innovation, and we recognize that it is the vigor and enthusiasm of young minds that often drive the most groundbreaking discoveries. We actively encourage students, early-career researchers, and scientists to submit their work and engage in meaningful discourse within the pages of our journal. We take pride in providing a platform for these emerging researchers to share their novel ideas and findings with the broader scientific community.

In today's rapidly evolving scientific landscape, it is increasingly evident that the challenges we face require a collaborative and interdisciplinary approach. The most complex problems demand a diverse set of perspectives and expertise. Integrative Omics and Applied Biotechnology (IIOAB) Journal has consistently promoted and celebrated this multidisciplinary ethos. We believe that by crossing traditional disciplinary boundaries, we can unlock new avenues for discovery, innovation, and progress. This philosophy has been at the heart of our journal's mission, and we remain dedicated to publishing research that exemplifies the power of interdisciplinary collaboration.

Our journal continues to serve as a hub for knowledge exchange, providing a platform for researchers from various fields to come together and share their insights, experiences, and research outcomes. The collaborative spirit within our community is truly inspiring, and I am immensely proud of the role that IIOAB journal plays in fostering such partnerships.

As we move forward, I encourage each and every one of you to continue supporting our mission. Whether you are a seasoned researcher, a young scientist embarking on your career, or a reader with a thirst for knowledge, your involvement in our journal is invaluable. By working together and embracing interdisciplinary perspectives, we can address the most pressing challenges facing humanity, from climate change and public health to technological advancements and social issues.

I would like to extend my gratitude to our authors, reviewers, editorial board members, and readers for their unwavering support. Your dedication is what makes IIOAB Journal the thriving scientific community it is today. Together, we will continue to explore the frontiers of knowledge and pioneer new approaches to solving the world's most complex problems.

Thank you for being a part of our journey, and for your commitment to advancing science through the pages of IIOAB Journal.

Yours sincerely,

Vasco Azevedo

Vasco Azevedo, Editor-in-Chief
Integrative Omics and Applied Biotechnology
(IIOAB) Journal

Prof. Vasco Azevedo
Federal University of Minas Gerais
Brazil

Editor-in-Chief

Integrative Omics and Applied Biotechnology (IIOAB) Journal Editorial Board:

ISSN: 0976-3104
REGULAR ISSUE
Chowbina S.

COMMENTARY OPEN ACCESS

TOWARDS TRANSLATIONAL SYSTEMS BIOLOGY AND PERSONALIZED MEDICINE IN CANCER

Sudhir Chowbina

Advanced Biomedical Computing Center, National Cancer Institute-Frederick/SAIC-Frederick Inc., Frederick, MD 21702

Corresponding author: Email: sudhir.chowbina@nih.gov, sudhir.cr@gmail.com; Tel: +011-301-846-7689; Fax: +011-301-846-5762

Received on: 12th-May-2011; **Revised on:** 10th-July-2011; **Accepted on:** 10th– July-2011; **Published on:** 1st –Jan-2012

[I] INTRODUCTION

Living cells are characterized by their ability to perceive and correctly respond to their microenvironment. This process is called cell signaling and it governs basic cellular activities and coordinates cell actions [1]. Signal transduction processes form the basis of cell growth, tissue repair, and immunity as well as normal tissue homeostasis. Distorted cell signals lead to diseases such as cancer, autoimmunity, and diabetes. By understanding cell signaling, can result in effective diagnostic and therapeutic solutions to treat diseases.

Cancer continues to cause a major public health crisis. According to the World Health Organization, cancer accounted for 7.6 million deaths (around 13% of all deaths) in 2008. Irrespective of the environmental factors involved in causing cancer, cell signaling is involved at some level. Cancer cell have a proliferative advantage because they deregulate, up-regulate or inhibit pathways and signaling is by default mechanistically involved in cell development.

Cancers are extremely robust [2], complex, heterogeneous diseases due to dynamic network behavior and signaling pathway crosstalk within the cell. The significance of genetic mutations in cancer development is emphasized by Hanahan & Weinberg where they refer to six critical changes in cell functioning that describes malignant cancer growth as the hallmarks of cancer. The following six changes incorporate some aspect of genetic mutation and evolutionary selection causing malignant progression: (a) self-sufficiency in growth signals; (b) insensitivity to anti-growth signals; (c) evading apoptosis; (d) limitless replicative potential; (e) sustained angiogenesis; and; (f) tissue invasion and metastasis [3]

Cancer is now not only a highly heterogeneous pathological condition but a multiscale problem [4]. The intimate connections between genes, signaling networks, subcellular organelles, and phenotypic traits are perturbed in a typical cancer cell. Cancer is defined by an extraordinary amount of heterogeneity among genes involved in tumorigenesis. If such a signaling network involving hundreds of proteins is disturbed or altered, a cancer phenotype could be generated. The genotypic and phenotypic variation makes understanding the processes driving tumorigenesis extremely challenging. To understand how signaling networks disrupt cellular behaviors causing cancer, it is necessary to use a systems approach.

Systems biology is an interdisciplinary field deriving concepts from the life sciences, engineering disciplines and computer science. This new field accentuates the functionality of all components working together and augments the traditional way of studying the individual roles of single components. Systems biology represents a quantitative approach to biology; thus demands collaborations between quantitative & non-quantitative disciplines and multidisciplinary teams [5].

High throughput technologies have led to detailed characterization of biochemical networks by allowing us to measure cellular components with few experiments. The challenge is to understand how cellular components are organized into a complex network based on the measurement of individual components, to understand causes of diseases and find effective drugs. The reconstruction and analysis of complex biological networks, such as metabolic networks, gene regulatory networks and protein-protein networks (PPN) are central topics of Systems Biology [6].

Incorporating and consideration for the multifunctionality of network components is important to fully comprehend biochemical pathways. Further, stoichiometric network reconstruction and associated mathematical analyses can be included to study genome-scale networks properties. Combining these analyses with experimental studies, new hypotheses can be generated about the interplay among the biochemical networks [7]

Systems biology is a unique integrative approach involving theoretical modeling and direct experimentation. Experiments provide data for model design and theoretical models provide insights into experimental observations, while the experiments confirm or refute model findings. Thus, multidisciplinary approach is ideal to understand systems biology. Researchers

THE IIOAB JOURNAL
ISSN: 0976-3104

from molecular biology, engineering, physics, computational science, statistics, chemistry, and mathematics need to cooperate in order to explain how the biological system work cooperatively and coherently [8].

Similar to interconnected roads in our cities, biomolecules inside cells are also networked. This suggests that biochemical pathways have cross-talk, which allows cancer to bypass the effects of a drug. Therefore, cancer needs to be treated with alternative molecular routes and target multiple genes. A systems perspective, rather than the current gene-centric view, could solve these issues and facilitate new options for cancer treatment and identify the most promising potential new drugs [9].

The systems biology approach integrates empirical, mathematical and bioinformatics techniques to understand the intricate biological and physiological processes. Systems biology helps by generating detailed blueprints depicting different kinds of cellular networks and by developing sophisticated mathematical, statistical and computational methods and tools to analyze these networks.

Understanding cancer requires development of mathematical models capable of generating testable predications and powerful hypotheses. In order to better understand cancer, a model must describe or accommodate the Weinberg's hallmarks of cancer. While focusing on these common aspects, mathematical modeling aims to contribute to the prevention, diagnosis and treatment of this complex disease.

CONFLICT OF INTEREST

The author declares no conflicts of interest.

REFERENCES

[1] Witzany G. (2000) Life, the communicative structure *: a new philosophy of biology*. Norderstedt: G. Witzany.
[2] Kitano H. (2004) Cancer as a robust system: implications for anticancer therapy. *Nat Rev Cancer* 4(3): 227–235.
[3] Hanahan D and Weinberg RA. (2000) The hallmarks of cancer. *Cell*, 100(1): 57–70.
[4] Rothschild Anderson AR and Quaranta V. (2008) Integrative mathematical oncology. *Nat Rev Cancer*, 8(3): 227–234.
[5] Tadmor B, and Tidor B. (2005) Interdisciplinary research and education at the biology-engineering-computer science interface: a perspective (reprinted article). *Drug Discovery Today* 10(23-24): 1706–1712.
[6] Ma HW, and Goryanin I. (2008) Human metabolic network reconstruction and its impact on drug discovery and development. *Drug Discovery Today* 13(9–10): 402–408.
[7] Gianchandani EP, Brautigan DL, and Papin JA. (2006) Systems analyses characterize integrated functions of biochemical networks. *Trends Biochem Sci* 31(5): 284-291.
[8] Hood L. (2003) Leroy Hood expounds the principles, practice and future of systems biology. *Drug Discov Today*, 8(10): 436–438.
[9] Wang E. (2010) Cancer Systems Biology (Vol. in press): Chapman & Hall/CRC Press.

ISSN: 0976-3104
REGULAR ISSUE
Mittal et al.

THE IIOAB JOURNAL

RESEARCH ARTICLE OPEN ACCESS

EXOGENOUS SURFACTANT PREVENTS THE MITOCHONDRIAL DEPOLARIZATION AND CHANGES IN CALCIUM HOMEOSTASIS DUE TO OXIDATIVE STRESS THAT LEADS TO APOPTOSIS IN EXPERIMENTAL LUNG INJURY

Neha Mittal and Sankar Nath Sanyal*

Department of Biophysics, Panjab University, Chandigarh-160014, INDIA

ABSTRACT

Background: *Apoptosis has been considered as an underlying mechanism in acute lung injury/acute respiratory distress syndrome. Recently, several alternative pathways such as the mitochondrial membrane depolarization for cell death have been discovered.* ***Objectives:*** *The present study investigated the role of surfactant therapy during LPS mediated changes in intracellular calcium concentration ([Ca]i) and mitochondrial depolarization as a possible intermediate in apoptosis.* ***Methods:*** *Adult male Sprague Dawley rats were divided into four groups: buffer controls; rats challenged with LPS (055:B5 E.coli); challenged with LPS and treated with porcine surfactant (P-SF); and challenged with LPS and treated with synthetic surfactant (S-SF). Experiments with surfactant were performed 72h after treatment with LPS.* ***Results:*** *To ascertain the mechanism of BALF cell apoptosis, we observed that LPS treatment induced oxidative burst, dissipated mitochondrial membrane potential, induced alteration of Ca^{2+} homeostasis and enhanced apoptosis. These effects were largely prevented by exogenous surfactant preparation.* ***Conclusion:*** *The anti-inflammatory activity may occur through an interaction with downstream signaling elements and Ca^{2+} influx. The findings show the importance of Ca^{2+} ions in regulating the response of BALF cells to oxidative stress that triggers downstream signaling cascades leading to the apoptosis. Therefore, treatments aimed at diminishing the damage to lung derived cells might become a key element in accelerating recovery and lead to the development of novel therapies for acute lung injury.*

Received on: 16-Dec-2010
Revised on: 10th-March-2011
Accepted on: 7th– April-2011
Published on: 15th –Jan-2012

KEY WORDS

ARDS; calcium homeostasis; mitochondrial membrane potential; ROS generation; surfactant; apoptosis

***Corresponding author:** Email: sanyalpu@gmail.com, sanyal@pu.ac.in; Tel: +91-0172-2534122

[I] INTRODUCTION

Acute lung injury (ALI) and its more severe form, acute respiratory distress syndrome (ARDS), represent a clinical syndrome that results from complex responses of the lung to a multitude of direct and indirect insults. The different types of cell death that occur and the underlying mechanisms utilized depend on both experimental and clinical conditions [1]. Lipopolysaccharide (LPS) induced acute lung injury generates reactive oxidative species, which induce complex cell death patterns composed of apoptosis, and necrosis.

Apoptosis is a process of cell death in which the cells undergo nuclear and cytoplasmic shrinkage; the chromatin is condensed and partitioned into multiple fragments, and finally the cells are broken into multiple membrane-bound bodies. In a number of experimental systems, disruption of mitochondrial transmembrane potential ($\Delta\Psi m$) constitutes a constant early event of the apoptotic process that precedes nuclear disintegration [2]. $\Delta\Psi m$ loss can be brought about by reactive oxygen species (ROS) added directly in vitro or generated by agents that affect cellular metabolism [3]. A number of molecular targets of reactive oxygen species (ROS) have been identified, including membrane phospholipids, transporters, enzymes, transcription factors, DNA, etc. [4]. Respiratory chain dysfunction could also lead to increased ROS production and formation of a vicious cycle, thereby killing cells either necrotically, apoptotically, or by some combination thereof [5]. Key features within the apoptosis cascades are dissipation of mitochondrial membrane potential, increased mitochondrial oxidant production, and apoptogenic protein release [6].

On the other hand, elevation of the cytosolic free Ca^{2+} ($[Ca^{2+}]_c$) level is suggested to participate in the activation of nucleases that are involved in chromatin organization, induce gene expression and also cleavage of nuclear DNA activated by nucleases during programmed cell death or apoptosis [7]. The role of elevated $[Ca^{2+}]_c$ in bringing about early apoptotic changes including $\Delta\Psi m$ loss in a cell is evident from studies showing the ability of intracellular Ca^{2+} chelators to block apoptosis [8] and the proapoptotic changes that can be induced by Ca^{2+}-mobilizing agents responsible for the release of Ca^{2+} from the endoplasmic reticulum [9]. In some cell systems, it is

THE IIOAB JOURNAL
ISSN: 0976-3104

not only the $[Ca^{2+}]_c$ increase but mitochondrial Ca^{2+} ($[Ca^{2+}]m$) overload [10] as well that precipitates a decrease in $\Delta\Psi m$.

Clinical investigations have demonstrated that replacement therapy with exogenous surfactant is effective for patients with ARDS [11]. Administration of surfactant *in vivo* inhibited the mitochondrial pathway of caspase-mediated apoptosis triggered by LPS [12] or by a variety of stimuli, such as inflammatory cytokines, growth factors, reactive oxygen species, and others, which are also involved in this model [13, 14]. Our earlier work has shown that surfactant therapy was proved to be effective during inflammatory responses in endotoxin induced ARDS [14, 15]. It seems reasonable therefore, that exogenous surfactant may improve surfactant function either by supplementing the lack of endogenous surfactant or by neutralizing the surfactant inhibitors, but the mechanism(s) on the effectiveness of exogenous surfactant on ARDS are not fully elucidated.

Together, the existing literature suggests that the alterations of Ca^{2+} levels in cell cytoplasm and mitochondria brought about by ROS or other agents can serve as critical signaling components leading to the activation of the apoptotic pathway. Therefore, we have focused our interest on the oxidative stress, mitochondrial membrane potential, cytosolic Ca^{2+} levels, and cell death seen in BALF cells in a rat model of ARDS induced by intratracheal instillation of LPS and subsequently treated with exogenous surfactant.

[II] MATERIALS AND METHODS

2.1. Animal modal

Male rats of Sprague Dawley (SD) strain, weighing 150-200g were taken from the Central Animal House of Panjab University and kept in polypropylene cages and supplied with pellet diet and drinking water ad libitum. Control animals were administered with 300µl of the buffer (50mM Tris-HCl, pH-7.4, 150mM NaCl, 1mM NaN3, 0.2mM PMSF). For LPS animals, endotoxin (150µg of 055:B5 E.coli LPS, Sigma Aldrich, USA) was suspended in 300µl of surfactant buffer. All rats were anesthetized with ketamine (130mg/kg. i.p.), such that they remained unconscious throughout the entire instillation procedure and had no cough reflex upon intubation. A small incision was made on the ventral region of the neck and the trachea carefully exposed. Animals were then placed on a slight incline, intubated with a 26-gauge needle and either buffer or LPS instilled followed by 2-3 boluses of 1ml air to facilitate the distribution of the instilled fluid. Shortly thereafter, when normal spontaneous breathing was apparent, the neck incision was closed with silk sutures. To avoid any infection betadine and neosporin powder were applied to the wound area. Two hours prior to killing, surfactant isolated from porcine (0.5mg protein + 0.86mg lipid/300µl) or synthetic surfactant (6.95mg lipid/300µl) were intratracheally instilled in P-SF and S-SF groups respectively, after LPS administration following the identical instillation procedure. The animals were sacrificed at 72 hours after buffer or LPS instillation [14]. All of the animal procedures as reported here had been carried out following the guidelines approved by the Panjab University Ethical Committee on the use of the experimental animals for biomedical research.

2.2. Surfactant preparation

Surfactant was isolated from porcine lung homogenate (P-SF) by sucrose density gradient method [16] while protein free synthetic surfactant (S-SF) was prepared with 13.9mg/ml dipalmitoylphosphohatidyl choline (DPPC), 1.5mg/ml hexadecanol and 1.0mg/ml Tyloxapol [16].

2.3. Bronchoalveolar lavage fluid (BALF) isolation

At the end of each experiment, a bronchoalveolar lavage was performed using 5ml phosphate buffered saline (PBS, pH-7.4). The average fluid recovery was greater than 90%. The recovered volume was centrifuged at 1000 rpm for 10 min at 40C and the supernatants were stored at -20^{0}C until analysis. Differential counts were performed on 200 cells stained with Wright Giemsa [13].

2.4. Measurement of intracellular ROS

To monitor the level of ROS, the cell-permeating probe DCFH-DA was used [14] whose fluorescence was found to be proportional to the amount of ROS formed intra-cellularly. Cells were incubated in dark conditions with the DCFH-DA dye (2.5µM) and with Hoechst 33342 for 15 min at 37^{0}C for counter staining and the cell suspension were placed on glass slide for observation under fluorescence microscope at 400 X (Axioscope, A1, Carl Zeiss, Germany).

2.5. Measurement of mitochondrial membrane potential changes

$\Delta\Psi m$ was estimated using JC-1 as a probe according to the method of Dey and Moraes [17] with slight modifications. Briefly, cells (1×10^6) were incubated for 7 min with 10µM of JC-1 at 37°C, washed, resuspended in PBS and measured for fluorescence in a fluorescence spectrometer. The ratio of the reading at 590 nm to the reading at 530 nm (590:530 ratio) was measured as the relative $\Delta\Psi m$ value. For microscopy, JC-1-stained cells were placed on slides and immediately imaged with the fluorescence microscope using the X40 objective. Aggregates of JC-1 are retained in intact mitochondria and fluoresce red, whereas mitochondria that have undergone a permeability transition release the JC-1 monomers into the cytoplasm, where they fluoresce green. Similarly, cells were incubated at 37^{0}C for 15 min with rhodamine 123 at a concentration of 10µM, washed and resuspended in PBS (pH-7.4), and measured for fluorescence at 488nm excitation and 536 nm emission. For microscopy, cells were incubated with dye, washed similarly as mentioned above and resuspended in 50µl PBS and placed on slides for viewing under fluorescence microscope at 400X.

2.6. Measurement of intracellular calcium mobilization

To evaluate whether LPS and surfactant cause mobilization of intracellular calcium, we used the fluorescent indicator chlortetracycline (CTC). CTC exists as neutral and ionic forms, and the anionic form complexes with cations (Ca^{2+}). An increase in fluorescence emission by up to two orders of magnitude occurs when CTC binds to the membrane-associated Ca^{2+}, as compared to the fluorescence of CTC alone. The cell suspension was incubated with 10µM CTC for 5 min at 37^{0}C using excitation 390 nm, emission 520 nm. Changes in luminal Ca^{2+} are expressed as changes in the intensity of CTC fluorescence [18]. For microscopy, cells were incubated with CTC and propidium iodide (as counter stain) and the 10µl suspension was placed on glass slide, covered with cover slip and observed under the fluorescence microscope.

THE IIOAB JOURNAL
ISSN: 0976-3104

2.7. Measurement of cytosolic free Ca^{2+} concentrations

Changes in intracellular Ca^{2+} concentration $[Ca^{2+}]i$ were monitored with the fluorescent probe FURA-2/AM as described by Grynkiewicz et al. [19] with slight modifications. Cells ($1x10^6$ /ml) were loaded with 1µM fura-2/AM (1µg/µl in DMSO) for 30 min at 37^0C, to allow loading of the dye. The cells were collected by centrifugation at 500 g for 10 min at 4^0C, and resuspended in the PBS (pH 7.4). Fluorescence measured at excitation wavelengths of 340nm and 380nm, and an emission wavelength of 510nm. Ratios (R) of fluorescence intensity (F) of F340/F380, were measured for which the fractional changes in $[Ca^{2+}]i$ determined [19]. The fluorescence after sequential addition of SDS (20%) and 0.5M EGTA (pH 8) to the cell suspension provided the maximum fluorescence ratio (Rmax) and minimum fluorescence ratio (Rmin), respectively. To convert fluorescence values into absolute $[Ca^{2+}]i$, calibration was performed at the end of each experiment. $[Ca^{2+}]i$ was calculated using the following equation: $[Ca^{2+}]i = Kd[(R-Rmin)/(Rmax-R)]$, [19] where Kd is the dissociation constant of the FURA-2 complex (225nM), and R is the ratio of the fluorescence intensities measured at 340 and 380nm. Rmax is the same ratio when saturated with Ca^{2+} (after the addition of SDS), while Rmin is the same ratio in the absence of Ca^{2+} (after the sequential addition of EGTA)

2.8. Quantification of apoptotic cells

An annexin V–fluorescein isothiocyanate (FITC) kit (TACS® Annexin V Kits, Trevigen Inc. Gaithersburg, MD) was used to quantify apoptotic cells in accordance with manufacturer's procedure and examined for Annexin V-fluorescein isothiocyanate and propidium iodide (PI) fluorescence under fluorescence microscope.

2.9. Statistical analysis

Statistical analysis was performed using SPSS version 10.0 software. One way analysis of variance (ANOVA) was done to compare the means between the different treatments using Post-Hoc comparison by Least Significant Difference (LSD) method. A value of $p < 0.05$ was considered significant in the present study. All data were expressed as Mean ± SD of five animals for each group.

[III] RESULTS

3.1. LPS generated oxidative burst

H_2DCFDA is a nonpolar compound that readily diffuses into the cells, where it is hydrolyzed to the nonfluorescent derivative dichlorodihydrofluorescein and is thereby trapped within the cells. In the presence of a proper oxidant, dichlorodihydrofluorescein is oxidized to the highly fluorescent 2,7-dichlorofluorescein. We analyzed the DCFH-DA stained cells with a fluorescence microscope for all the treatment groups. **Figure– 1(a)** shows the morphological changes that occur in the BALF cells after exposure to the oxidative stress. 13.25% of the control cells fluoresce blue due to the uptake of Hoechst 33342 dye, indicating less oxidative stress. After exposure to LPS, an increased number of cells show a heterogeneous staining pattern and 73.2% ($p<0.001$) of the cells show DCFH-DA dye uptake and fluoresce green (indicated with arrows), whereas 34.25% ($p<0.001$) of cells were seen positive in LPS+P-SF group and 46.5% ($p<0.001$) of cells in LPS+S-SF group which means the oxidative stress is less prevalent in surfactant treated groups as compared to the LPS treated group **[Figure– 1b]**.

3.2. Changes in mitochondrial membrane potential

JC-1 is a cationic mitochondrial dye that is lipophilic and becomes concentrated in the mitochondria in proportion to their ΔΨm; more dye accumulates in mitochondria with greater ΔΨm and ATP-generating capacity. Therefore, the fluorescence of JC-1 can be considered as an indicator of relative mitochondrial energy state. The dye exists as a monomer at low concentrations (emission 530 nm, green fluorescence) but at higher concentrations forms J-aggregates (emission 590 nm, red fluorescence). Exposure to LPS induced a significant reduction (1.13 ± 0.04, $p<0.001$) of mitochondrial membrane potential in BALF cells when compared with control rats (10.72 ± 0.86, **Figure– 2b**). Accumulation of JC-1 dye in the aggregated form (red fluorescence) was observed in the mitochondria of control cells **[Figure– 2a]**. In contrast, after exposure to LPS monomeric dye dispersed in the cytoplasm and displayed green fluorescence indicating the collapse of mitochondrial membrane integrity. Surfactant treated groups had a distinct pattern of staining with areas of both red and green that overlapped as yellow indicating a very close placement of regions with high and low ΔΨm. Cytoplasmic appearance of monomeric JC-1(green fluorescence) seen in the LPS+ surfactant group was less prevalent (6.73 ± 0.69 in P-SF group and 3.85 ± 0.35 in S-SF, $p<0.001$) than that detected in LPS treated animals.

Rhodamine fluorescence was clearly seen in control and surfactant treated cells **[Figure–2c]**. The fluorescence intensity is significantly decreased by LPS administration (11.74 ± 1.45, $p<0.001$) which is reverted back up to the control level by surfactant treatment (control = 22.69 ± 0.64; P-SF = 20.14 ± 0.20; S-SF = 18.11 ± 0.44, $p<0.001$, **Figure– 2d**).

3.3. Alterations in Ca^{2+} homeostasis

The fluorescence emission of CTC has been used to measure the level of divalent cations (specifically Ca^{2+} and Mg^{2+}) associated with envelope membranes in a wide range of animal cells. Images illustrating the cells taking up CTC dye (green fluorescence) in all the groups were shown in **Figure 3(a)**. Quantitative analysis showed 35.5% ($p<0.001$) of cells were CTC positive in LPS group as compared to 6.5% CTC positive cells in control group **[Figure– 3c]**. Both LPS+SF treated groups showed decreased percentage of CTC positive cells when comparisons were made with LPS group (20.25% in LPS+P-SF ($p<0.001$) and 21.25% ($p<0.001$) in LPS+P-SF).

The fluorescence signal was diminished significantly with LPS treatment (1.78 ± 0.39, $p<0.001$) in comparison to control group (4.40 ± 0.60) which indicates more Ca^{2+} displaced from the cell

THE IIOAB JOURNAL
ISSN: 0976-3104

membrane to the cytosol with LPS whereas CTC bind to the membrane bound Ca^{2+} in control group (high fluorescence intensity, **[Figure– 3b]**. In surfactant treated groups, the LPS mediated fluorescence intensity was gradually increased with P-SF (3.05 ± 0.24, $p<0.001$) and S-SF (2.45 ± 0.11, $p<0.001$). Further, in this study the cytosolic Ca^{2+} concentration was measured in BALF cells with LPS treatment followed by exogenous surfactant (P-SF and S-SF). In contrast to control group ($[Ca^{2+}]i$ = 50.12 ± 1.51 nM), LPS induced a gradual increase in $[Ca^{2+}]i$ (199.49 ± 0.96 nM, $p<0.001$) which is also consistent with the above result. In the presence of exogenous surfactants, the LPS-induced increase in $[Ca^{2+}]i$ was reduced by P-SF (143.95 ± 1.62 nM, $p<0.001$). Similarly, the LPS-induced $[Ca^{2+}]i$ was also markedly inhibited by the S-SF (172.28 ± 0.82 nM, $p<0.001$) as shown in **Figure– 3(d)**.

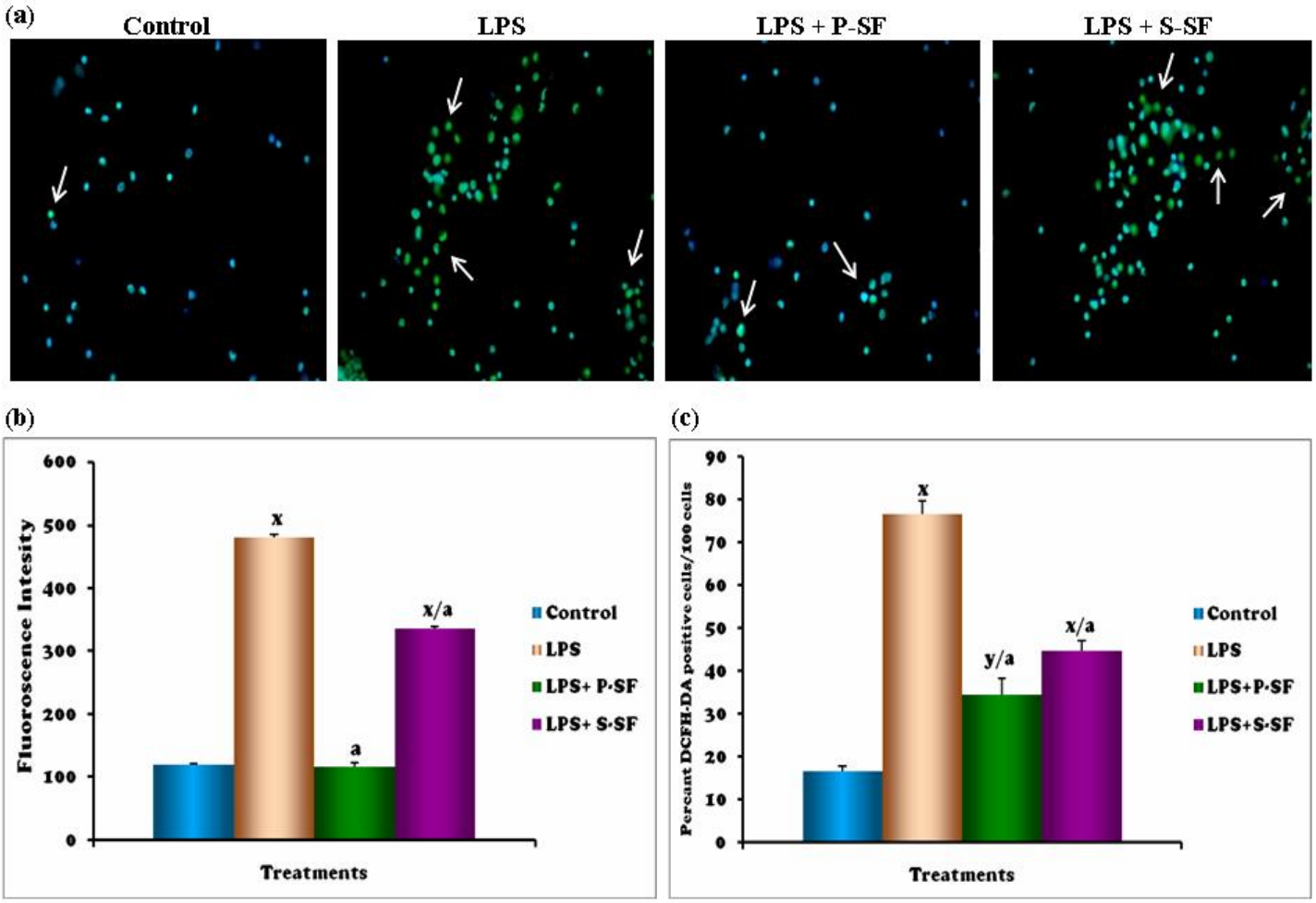

Fig. 1: (a) Images depict the morphological changes with the DCFH-DA dye in all the groups. **(b)** Quantitative analysis showed DCFH-DA positive cells. Values are mean ± S.D. of four independent observations, $^{x}p<0.001$ vs control; $^{a}p<0.001$ vs LPS.

3.4. Apoptosis by fluorescent dyes

Annexin V was used in conjunction to the vital dye propidium iodide (PI) to distinguish the apoptotic cells from necrotic or late stage apoptotic cells **[Figure– 4a]**. Based on binding of annexin V and PI, cells can be divided into three subpopulations, i.e. early apoptotic cells (annexin V positive, PI negative), late apoptotic cells (annexin V positive, PI positive) and necrotic cells (PI positive). In the LPS treatment group 54.25% of cells were positive for cell surface exposure of PS which mark them for early apoptosis **[Figure– 4b]** whereas only 13% apoptotic cells were found in control cells and many were PI positive. Mixed population of dual staining cells was seen with surfactant co-administration. The percentages of annexin V positive cells were reduced to 27.25% ($p<0.001$) in P-SF and to 33.5% ($p<0.001$) in S-SF group in comparison to LPS treatment.

THE IIOAB JOURNAL
ISSN: 0976-3104

[IV] DISCUSSION

Reactive oxygen species (ROS) have been implicated in a variety of pulmonary diseases including adult respiratory distress syndrome [20]. We examined ROS production in BALF cells using a fluorescent dye (DCFH-DA) and found that both the surfactants inhibited LPS stimulated ROS generation which is consistent with previous results as found in the rabbit alveolar macrophages [21]. This would suggest that surfactant has the inhibitory effects on the immediate inflammatory response. Similarly, in studies with natural surfactant with SP-B and SP-C versus synthetic surfactant both the surfactant types equally inhibited the human neutrophil respiratory burst [22]. In addition to causing direct injury to lung associated cells, ROS also involved in the regulation of signaling activity [23].

Mitochondria are primary sources of ROS inside the cells and in the course of signal transduction that leads to apoptosis, mitochondria may release pro-apoptotic molecules, which is accompanied by loss of the transmembrane potential ($\Delta\Psi m$) that can be detected by specific fluorescent probes [24]. Freshly isolated BALF cells showed a complex staining with JC-1, indicating an intricate network of mitochondrial structures exhibiting both red (high membrane potential) fluorescence and green (low mitochondrial membrane potential). The ratio of red to green fluorescence is a measure of the mitochondrial membrane potential. This pattern of regions of hyperpolarized and depolarized mitochondria has been reported in other cell types and is considered to reflect uneven distribution of proton circuits, respiration, ATP synthesis, and localized Ca^{2+} inside mitochondria [25].

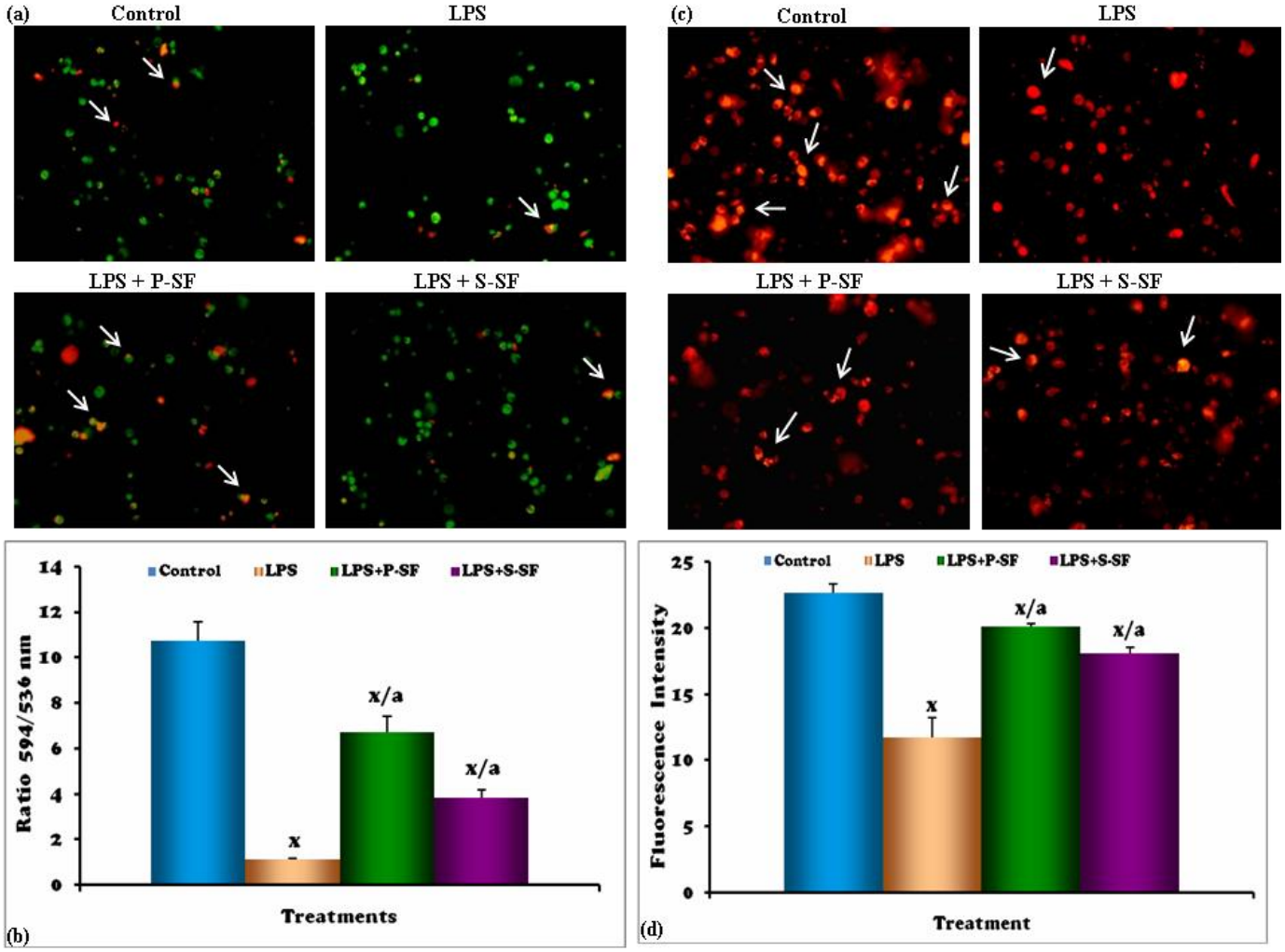

Fig. 2: (a) Changes in morphology of mitochondrial integrity in control, LPS-treated cells and with LPS + surfactant treatment precede **(b)** changes in mitochondrial membrane potential with JC-1. **(c)** Images with rhodamine-123 whereas **(d)** represents results from fluorometric analysis with rhodamine-123. Values are mean ± S.D. of four independent observations, $^{x}p<0.001$, $^{y}p < 0.01$ vs control; $^{a}p<0.001$ vs LPS.

THE IIOAB JOURNAL
ISSN: 0976-3104

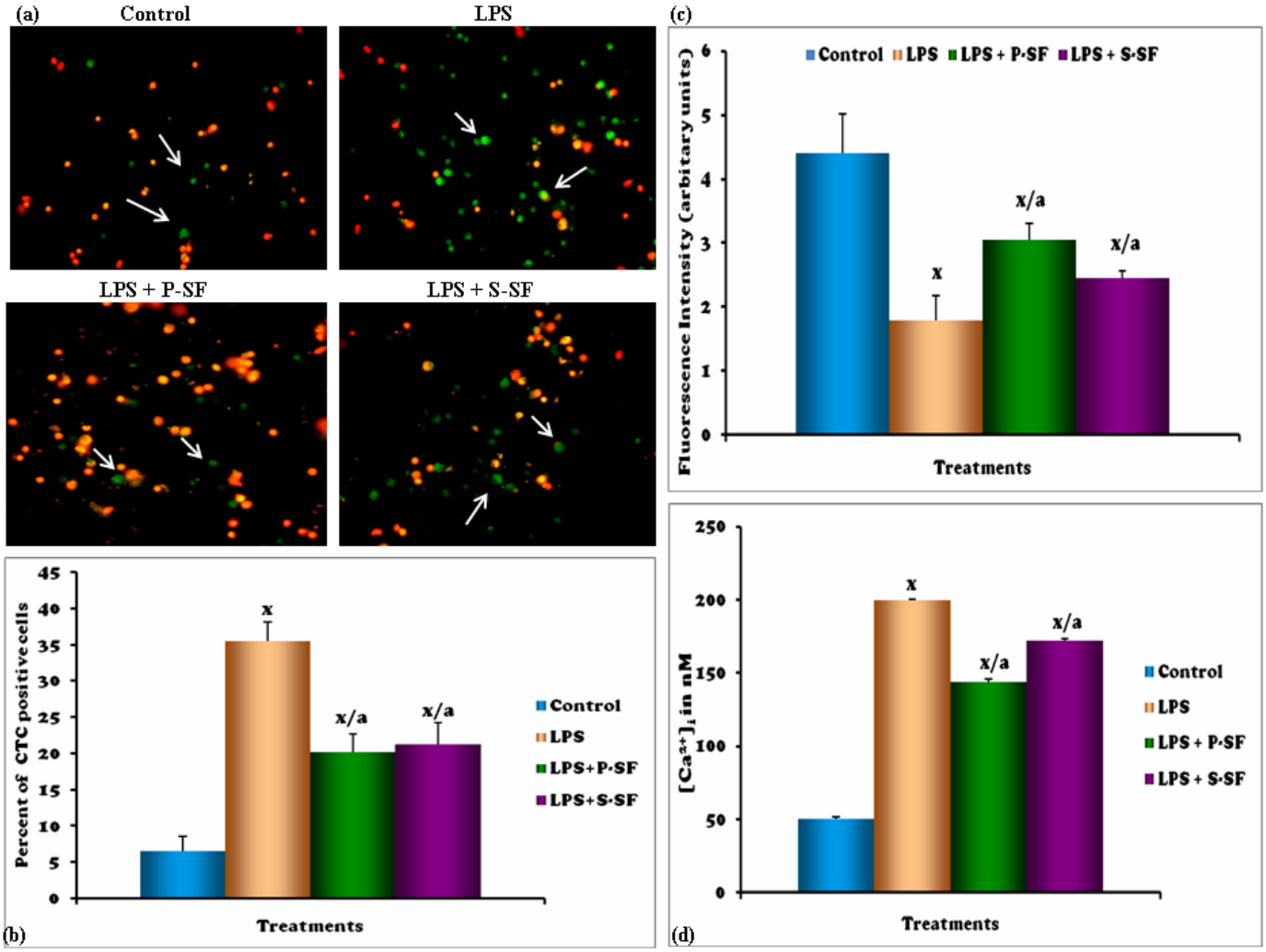

Fig. 3: (a) Images depict the effect of various treatments on CTC fluorescence. **(b)** Alterations in Ca^{2+} mobilization as measured with CTC fluorescence and **(c)** percentage of CTC positive cells/100 cells from four independent observations in each group **(d)** Intracellular calcium (nM) in BALF cells after LPS and surfactant treatments. Values are mean ± S.D. of four independent observations, $^{x}p<0.001$ vs control; $^{a}p<0.001$ vs LPS.

Mitochondrial dysfunction may also result through a change in cation homeostasis brought about by high ROS levels [26]. There are several lines of evidence to support strong role of Ca^{2+} [27]. CTC is a fluorescence-based stain, which forms chelate complexes in the presence of calcium ions in a 1:1 ratio [28]. When the CTC-calcium complex is mobilized from the highly lipophilic membrane environment to the more polar cytosol, there is a 100 fold decrease in the quantum efficiency of the indicator, which leads to a decrease in the observed fluorescence signal [29]. Calcium is released from the endoplasmic reticulum stores on stimulation of the cell, leading to a calcium influx across the plasma membrane via calcium channels [30]. Various pathogenic particles have been shown to produce changes in calcium flux within the cell [31] and a large number of physiological and pathological cellular functions could be stimulated via calcium signaling. The release of pro-inflammatory mediators such as the cytokine TNF-α is driven by intracellular calcium related signaling pathways in diseases such as sepsis [32].

In the present study, the LPS treatment induces an elevation in $[Ca^{2+}]i$ in the BALF cells and such Ca^{2+} influx was inhibited by both animal derived and synthetic surfactants. Surfactant also inhibits Ca^{2+} influx in human neutrophils, possibly by membrane depolarization from insertion of surfactant-associated protein-dependent cation channels [33]. More recently, bovine-derived surfactants were found to directly increase neutrophil $[Ca^{2+}]i$ by releasing Ca_2+ from internal

THE IIOAB JOURNAL
ISSN: 0976-3104

stores [34]. Therefore, blocking extracellular Ca^{2+} influx previously shown to modulate inflammatory response in peritoneal macrophages [35] may be an important mechanism regulating the anti-inflammatory properties of the exogenous surfactants. As measured in other trials, the phospholipids from both animal-derived and synthetic-surfactants demonstrate anti inflammatory properties. DPPC, the major phospholipid in natural and exogenous surfactants, similarly inhibited Ca^{2+} influx in the NR8383 AM cell line in an earlier study [36].

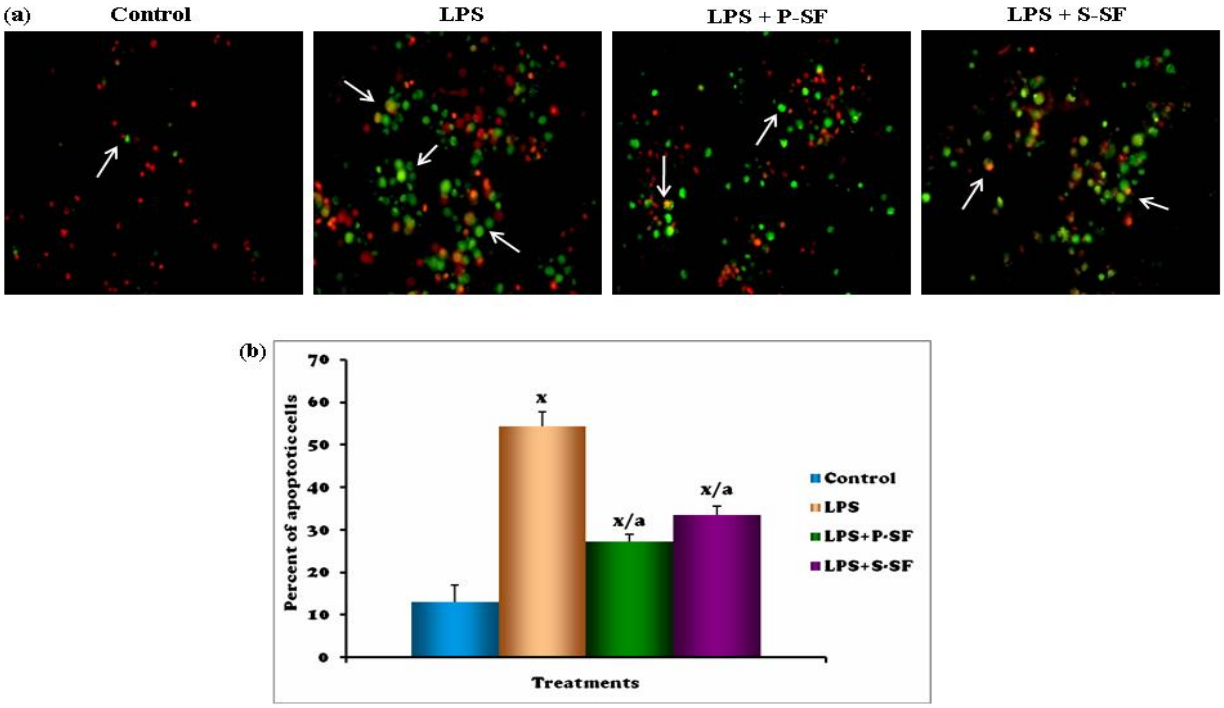

Fig. 4: (a) Photomicrograph showing apoptotic cells by staining with Annexin V and propidium iodide. **(b)** Quantitative analysis of the apoptotic cells, total 100 cells were counted in four different slides from each group and percent of apoptotic cells calculated. Values are mean ± S.D. of four independent observations, $^{x}p < 0.001$vs control rats and $^{a}p < 0.001$ vs LPS rats.

[V] CONCLUSION

In conclusion, the explanation of the loss ΔΨm, associated with an increase in $[Ca^{2+}]_c$ is that H_2O_2 is placing stress on cellular energy store by driving down the ATP levels that would drive ATP synthesis and run down the electrochemical gradient. The Ca^{2+} influx coupled with release of Ca^{2+} from intracellular pools may provide a signal for the loss of ΔΨm that eventually leads to apoptosis-like death in LPS mediated ARDS model. Because mitochondrial changes brought about by ROS could be a crucial event in the pathogenesis of the disease, the effects of exogenous surfactant on elements in this signal transduction pathway may clarify its role of minimizing pulmonary inflammation associated with the ARDS.

ACKNOWLEDGEMENT

This work is supported by grant from Indian Council of Medical Research (ICMR), New Delhi (Ref. No. 61/5/2005-BMS).

CONFLICTS OF INTERESTS

The authors report no conflicts of interest. The authors alone are responsible for the content and writing of the paper.

REFERENCES

[1] Tang PS, Mura M, Seth R, Liu M. [2008] Acute lung injury and cell death: how many ways can cells die? *Am J Physiol Lung Cell Mol Physiol* 294:L632–L641.

[2] Zamzami N, Marchetti P, Castedo M, Hirsch T, Susin SA, Masse B, Kroemer G. [1996] Inhibitors of permeability transition interfere with the disruption of the mitochondrial transmembrane potential during apoptosis. *FEBS Lett* 384:53–57.

[3] Dvorakova K, Waltmire CN, Payne CM, Tome ME, Briehl MM, Dorr RT. [2001] Induction of mitochondrial changes in myeloma cells by imexon. *Blood* 11:3544–3551.

[4] Thannickal VJ, Fanburg BL. [2000] Reactive oxygen species in cell signaling. *Am J Physiol Lung Cell Mol Physiol* 279:L1005–L1028.

THE IIOAB JOURNAL
ISSN: 0976-3104

[5] Ide T, Tsutsui H, Hayashidani S, Kang D, Suematsu N, et al. [2001] Mitochondrial DNA damage and dysfunction associated with oxidative stress in failing hearts after myocardial infarction. *Circ Res* 88:529–535.

[6] Mayer B, Oberbauer R. [2003] Mitochondrial regulation of apoptosis. *News Physiol Sci* 18:89–94.

[7] Tagliarino C, Pink JJ, Dubyak GR, Nieminen AL, Boothman DA. [2001] Regulation of the p53 tumor suppressor protein. *J Biol Chem* 276:19150–19159.

[8] Kruman II, Mattson MP. [1999] Pivotal role of mitochondrial calcium uptake in neural cell apoptosis and necrosis. *J Neurochem* 72:529–540.

[9] Koya RC, Fujita H, Shimizu S, Ohtsu M, Takimoto M, Tsujimoto Y, Kuzumaki N. [2000] Gelsolin Inhibits Apoptosis by Blocking mitochondrial Membrane Potential Loss and Cytochrome c Release. *J Biol Chem* 275:15343–15349.

[10] Ward MW, Rego AC, Frenguelli BG, Nicholls DG. [2000] Mitochondrial membrane potential and glutamate excitotoxicity in cultured cerebellar granule cells. *J Neurosci* 20:7208–7219.

[11] Enhorning G. [1989] Surfactant replacement in adult respiratory distress syndrome. *Am Rev Respir Dis* 140:281–283.

[12] Spragg RG. [1995] Clinical results after natural and artificial exogenous surfactant therapy. *Appl Cardiopulm Pathophysiol* 5:116.

[13] Mittal N, Sanyal SN. [2010] Intratracheal Instillation of Surfactant Inhibits Lipopolysaccharide-induced Acute Respiratory Distress Syndrome in Rats. *Am J Biomed Sci* 2:190 – 201.

[14] Mittal N, Sanyal SN. [2009] Exogenous surfactant suppresses inflammation in experimental endotoxin-induced lung injury. l *J Enviorn Toxicol Pathol Onco* 28:341-349.

[15] Mittal N, Sanyal SN. [2010] Cyclooxygenase inhibition enhances the effects of surfactant therapy in endotoxin induced rat model of ARDS. *Inflammation* DOI: 10.1007/s10753-010-9211-6.

[16] Mittal N, Sanyal SN. [2010] Immunomodulatory properties of exogenous surfactant in adult rat alveolar macrophages. *Immunopharm Immunot* 32:153–159.

[17] Dey R, Moraes CT. [2000] Lack of Oxidative Phosphorylation and Low Mitochondrial Membrane Potential Decrease Susceptibility to Apoptosis and Do Not Modulate the Protective Effect of Bcl-xL in Osteosarcoma Cells. *J Biol Chem* 275:7087–7094.

[18] Dixon D, Brandt N, Haynes DH. [1984] Chlortetracycline fluorescence is a quantitative measure of the free internal Ca2+ concentration achieved by active transport. *J Biol Chem* 259:13737-13741.

[19] Grynkiewicz G, Poenie M, Tsien RY. [1985] A new generation of Ca_2+ indicators with greatly improved fluorescent properties. *J Biol Chem* 260:3440–3450.

[20] Hoidal JR. [2001] Reactive oxygen species and cell-signaling. *Am J Respir Cell Mol Biol* 25:661–663.

[21] Hayakawa H, Myrvik QN, St. Clair RW. [1989] Pulmonary surfactant inhibits priming of rabbit alveolar macrophage. Evidence that surfactant suppresses the alveolar macrophage in infant rabbits. *Am Rev Respir Dis* 140:1390–1397.

[22] Ahuja A, Oh N, Chao W, Spragg RG, Smith RM. [1996] Inhibition of the human neutrophil respiratory burst by native and synthetic surfactant. *Am J Resp Cell Mol Biol* 14:496–503.

[23] Sen CK, Packer L. [1996] Antioxidant and redox regulation of gene transcription. *FASEB J* 10:709–720.

[24] Cossarizza A, Kalashnikova G, Grassilli E, Chiappelli F, Salvioli S, Capri M, Barbieri D, Troiano L, Monti D, Franceschi C. [1994] Mitochondrial modifications during rat thymocyte apoptosis: a study at the single cell level. *Exp Cell Res* 214:323–330.

[25] Minamikawa T, Williams DA, Bowser DN, Nagley P. [1999] Mitochondrial permeability transition and swelling can occur reversibly without inducing cell death in intact human cells. *Exp Cell Res* 246:26–37.

[26] Duchen MR. [2000] Mitochondria and calcium: from cell signalling to cell death. *J Physiol* 529: 57–68.

[27] Hotchkiss RS, Osborne DF, Lappas GD, Karl IE. [1995] Calcium antagonists decrease plasma and tissue concentrations of tumor necrosis factor-α,interleukin-1β and interleukin-1α in a mouse model of endotoxin. *Shock* 3:337–432.

[28] Caswell AH, Hutchison JD. [1971] Selectivity of cation chelation to tetracyclines: evidence for special conformation of calcium chelate. *Biochem Biophys Res Commun* 43:625–630.

[29] Luthra R, Olson MS. [1978] The effects of chlorotetracycline on calcium movements in isolated rat liver mitochondria. Arch Biochem *Biophys* 191:494–502.

[30] Hoyal CR, Giron-Calle J, Forman HJ. [1998] The alveolar macrophage as a model of calcium signalling in oxidative stress. *J Toxicol Enviorn Health B Crit Care Rev* 1:117–134.

[31] Stone V, Brown DM, Watt N, Ritchie H, Wilson M, Donaldson K. [2000] Ultrafine particle-mediated activation of macrophages: intracellular calcium signalling and oxidative stress. *Inhale Toxicol* 12:345–351.

[32] Sayeed MM. [1996] Alterations in calcium signaling and cellular responses in septic injury. *New Horizons* 4:72–86.

[33] Chacon-Cruz E, Buescher ES, Oelberg DG. [2000] Surfactant Modulates Calcium Response of Neutrophils to Physiologic Stimulation via Cell Membrane Depolarization. *Pediatr Res* 47:405–413.

[34] Boston ME, Frech GC, Chacon-Cruz E, Buescher ES, Oelberg DG. [2004] Surfactant releases internal calcium stores in neutrophils by G protein-activated pathway. *Exp Bio Med* 229:99–107.

[35] Hotchkiss RS, Bowling WM, Karl IE, Osborne DF, Flye MW. [1997] Calcium antagonists inhibit oxidative burst and nitrite formation in lipopolysaccharide-stimulated rat peritoneal macrophages. *Shock* 8:170–178.

[36] Kerecman J, Mustafa SB, Vasquez MM, Dixon PS, Catro R. [2008] Immunosuppressive properties of surfactant in alveolar macrophage NR8383. *Inflamm Res* 57:118-125.

ISSN: 0976-3104
REGULAR ISSUE
Chavan and Bhongade

THE IIOAB JOURNAL

CASE REPORT | OPEN ACCESS

SOFT TISSUE RIDGE AUGMENTATION IN MAXILLARY ANTERIOR REGION BY USING DOUBLE FOLD PALATAL CONNECTIVE TISSUE PEDICLE GRAFT- A CASE REPORT

Ramesh Chavan[1*] and Manohar Bhongade[2]

[1] Dept. of periodontics and implantology,Maitri dental college and research centre, Anjora Durg, Chattisgarrh, INDIA
[2]Dept. of periodontics and implantology,Sharad pawar dental college,Deemed university, Sawangi (meghe), Wardha, 442001, Maharashtra, INDIA

ABSTRACT

Background: *The evolution of periodontal plastic surgical techniques allowed the clinician to meet growing expectations and demands of today's dental patient. Newer techniques are evolving in restorative dentistry and periodontics to treat these defects to improve the esthetics, form and functions of the dentition.* ***Aims:*** *To evaluate the outcome of double fold palatal connective tissue pedicle graft in Class III ridge defect in esthetic region.* ***Case description:*** *A 35-year old man presented with localized alveolar ridge deformity in maxillary anterior region was treated by double fold palatal connective tissue pedicle graft. Six months post surgically, soft tissue ridge augmentation resulted in 100% restoration of deficient ridge in anterior dentition.* ***Discussion:*** *Long term growth and development of clinical research in soft tissue and hard tissues has been provided a means of treating problems of inadequate alveolar ridges necessary for restorative procedures. Multiple surgical procedures may required to achieve predictable results. The technique described in this case report allows the graft to be folded before it is placed under the vestibular flap, favoring the gain in tissue volume with promising results without any postsurgical complication.* ***Conclusion:*** *soft tissue ridge augmentation resulted in 100% restoration of Class III ridge defect in anterior dentition.* ***Clinical significance:*** *As the thickness of connective tissue graft is limited in anterior palatal region, this technique is predictable for all types of ridge defects and can be used for routine patients.*

Received on: 30-March-2011
Revised on: 24th-July-2011
Accepted on: 12th– Sept-2011
Published on: 31st –Jan–2012

KEY WORDS

Ridge Augmentation, Pedicle Connective Tissue Graft, Esthetics

***Corresponding author:** Email: drrameshperio@gmail.com; Tel: 09503529926; Fax: 07152 287731

[I] BACKGROUND

A localized alveolar defects are frequently found in partially edentulous patients that impairs the prosthetic restoration of damaged ridge area causing esthetic, phonetic, and oral hygiene complications. These defects are associated with the deficit in volume of bone and soft tissues within the alveolar process resulting from traumatic tooth extractions, advanced periodontal diease or periapical pathologies, developmental defects, external trauma, and tumors. Siebert (1983) 1 identified three basic ridge deformities- Buccolingual loss of tissue (class I), Apicocoronal loss of tissue (class II) and combination of Buccolingual–Apicocoronal loss of tissue (class III).

Over the last decade, advancements and modifications in technologies in the field of restorative dentistry and periodontics have been able to achieve best results to restore form, function and esthetics of the patient. Reconstructive procedures for the deformed alveolar ridge have evolved guided bone regeneration 2, 3, 4, 5, 6, 7, bone graft and soft tissue graft beneath the flap or in tunnel made in the damaged ridge area 8,9,10. Soft tissue graft employed for ridge augmentation include use of free gingival or onlay graft, using the palate as a donor area, as proposed by Seibert and subepithelial connective tissue graft implanted in a tunnel or pouch prepared in the mucosa that lines the defect. However, each procedure presents certain limitations.

New techniques are constantly being developed to treat alveolar ridge defects. Gasparini (2004) 11 proposed a surgical procedure to treat localized alveolar ridge defects in posterior segment by using "double-fold connective tissue pedicle graft." Therefore, the purpose of this case report was to clinically evaluate the effectiveness of double-fold connective tissue pedicle graft to augment localized alveolar ridge defect in anterior dentition.

THE IIOAB JOURNAL
ISSN: 0976-3104

[II] CASE DISCRIPTION

A 35-year old man presented with localized alveolar ridge deformity in maxillary anterior region as a result of the extraction of the right central incisor due to trauma 1 year earlier. A clinical examination of the maxillary alveolar ridge revealed a Seibert Class III defect (combined apicocoronal, **Figure– 1**, and buccolingual, **Figure– 2**, loss of tissue height). A localized ridge augmentation was necessary to obtain esthetic prosthetic reconstruction and then it was decided to augment the ridge with double fold connective tissue pedicle graft. A provisional restoration was made prior to the surgery. The shape of the teeth, an axial inclination, emergence profile of the teeth and the embrasure form for provisional restoration were exact prototype of the final prosthesis was constructed. The provisional prosthesis was used to help in shaping the outline of the augmented ridge to the desired form during healing. Informed consent was obtained from the patient.

Immediately prior to the surgical procedure the patient was instructed to rinse for 30 seconds with 0.2% chlorhexidine gluconate solution. The area subjected to surgery was anaesthetized by nerve block and infiltration anaesthesia using local anaesthetic solution 2% Xylocaine with 1:1, 00, 000 epinephrine. The technique involved reflection of a thin epithelial connective tissue flap toward the palate for exposing underlying connective tissue **[Figure– 3]**. A full-thickness vertical incision was made from the mesial aspect of the crest of the deformed ridge toward the palatal aspect. The length of the incision was depending on the length of connective tissue graft desired. The palatal incision met a partial-thickness horizontal incision made on the crest of the edentulous ridge. An intracrevicular incision palatal to the right lateral incisor and canine was made while preserving the central papilla. The reflection of a thin epithelial connective tissue flap was initiated at the crest of an edentulous ridge to expose the underlying connective tissue. The desired graft was then outlined by the first vertical incision made along the mesial extent and full-thickness incisions were made along the mesial and distal extent of defect extending in such a way that the mesiodistal size of graft exceeds almost double the mesiodistal size of the ridge defect. Then, the connective tissue graft was reflected by blunt dissection with a back-action periosteal elevator **[Figure– 4]**. The reflection of palatal connective tissue graft was initiated at the apical or medial end, reflecting further coronally to reach the crest of the ridge defect. From the ridge crest, sharp dissection was performed near the periosteum to create a pouch **[Figure– 5]** between the alveolar mucosa and underlying bone on medial surface. The distal half of the connective tissue graft was then folded below the mesial half, giving rise to the first fold. With the help of a resorbable suture from the labial surface, the whole graft was rolled into the labial pouch, giving rise to the second fold. The graft was secured with the same suture **[Figure– 6, – 7]**. The palatal epithelial-connective tissue flap was replaced on the denuded bone and secured with nonresorbable sutures **[Figure– 8]**.

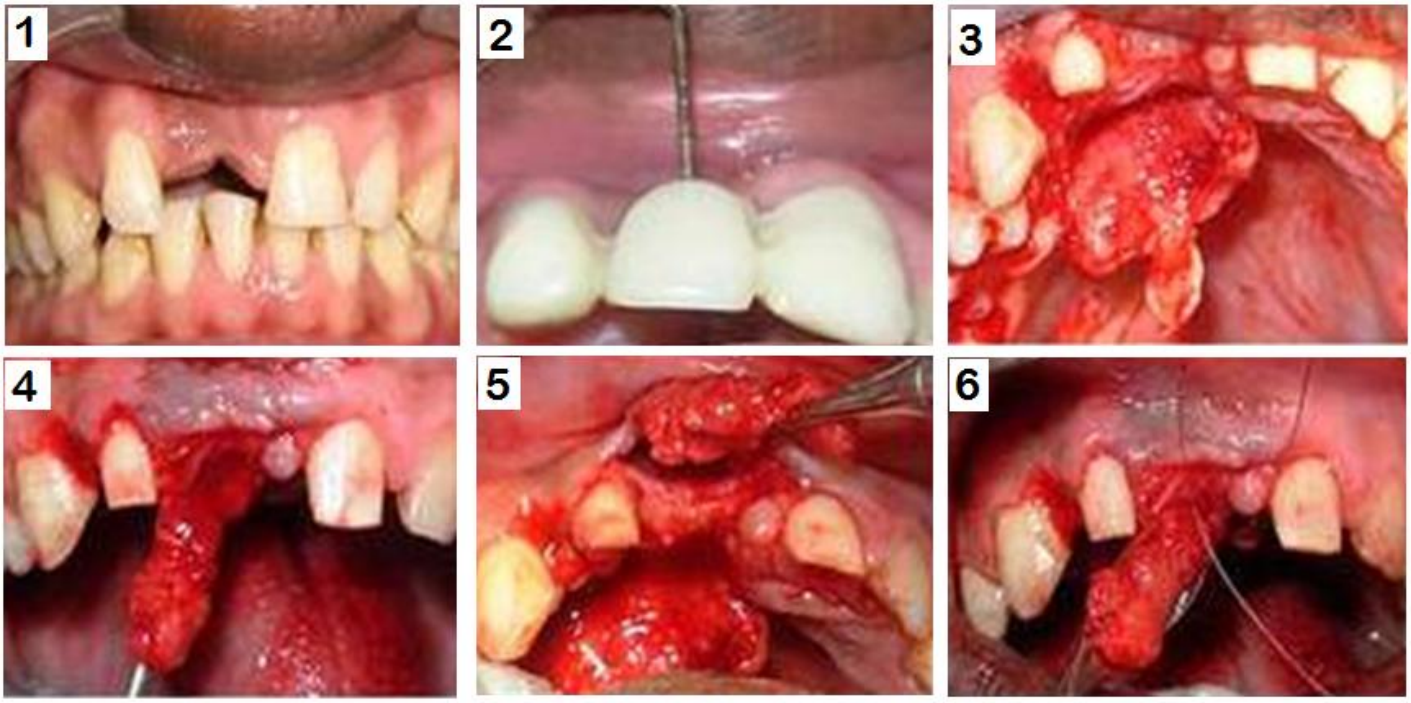

THE IIOAB JOURNAL
ISSN: 0976-3104

After surgery, a non-steroidal anti-inflammatory (Tab Ibugesic-Ibuprofen+Paracetamol, tds for 5 days) and antibiotic coverage consisting of Amoxicillin 500 mg tid was prescribed for 5 days. Patient instructed not to brush the teeth in the treated area and placed on 0.2% chlorhexidine gluconate mouthwash (Hexidine–ICPA) twice daily, for one minute, for 4-6 weeks. The sutures were removed 10 days after the periodontal surgery, and the patient presented with a satisfactory soft tissue healing.

During the course of the study, wound healing was uneventful. There were no post-operative complications and patient was satisfied with the results. The increase in the amount of tissue present was adequate to permit placing an esthetic fixed restoration. Initially shrinkage of soft tissue graft occurred but appeared stable thereafter.

Six months postsurgically, there was 4mm gain in buccolingual width with 1.5mm gain in apicocoronal hight. Augmentation resulted in 100% restoration of deficient ridge, with satisfactory improvement in buccolingual and apicocoronal direction **[Figure– 9]**. The construction of fixed restoration was delayed for 2 months. The final esthetics after placement of fixed restoration was acceptable to the patient with superior esthetic results **[Figure– 10]**.

[III] DISCUSSION

The case presented refers to the treatment of a Class III alveolar crest defect that involved the area of only one tooth, with satisfactory result. Several therapeutic alternatives have been proposed to correct this type of ridge defects. The previous techniques for ridge augmentation proposed by Abrams12 and Scharf and Tarnow13 used for the treatment of small to moderate Class I defects. These techniques pose difficulty in obtaining required volume because of limited thickness and size of the graft. At the same time, the techniques that involve large graft, such as full-thickness onlay grafts are more prone to cause necrosis10. In all these techniques, the mesiodistal dimension of the graft matches the mesiodistal dimension of the defect at the time of surgery; however, soft tissue graft undergoes shrinkage. Therefore, multiple surgical procedures may require to achieve predictable results1, 14, 15. The technique described in this case report was proposed by Gaspirani 11 and allows the graft to be folded before it is placed under the vestibular flap, favoring the gain in tissue volume. Since, the blood supply to the graft is guaranteed; the risk of necrosis is very low. Furthermore, clinically good color match was presented to the adjacent tissues, with less patient discomfort because of a single surgical site.

[IV] CONCLUSION

In this case report, ridge augmentation by using double fold palatal connective tissue pedicle graft showed satisfactory results in an esthetic region with a single surgical procedure that overcomes the limitations of the other soft tissue graft techniques. Clinical studies using large sample size with long-

THE IIOAB JOURNAL
ISSN: 0976-3104

term analysis are necessary to determine the success rate and predictability of this surgical technique.

[V] CLINICAL SIGNIFICANCE

As the thickness of connective tissue graft is limited in anterior palatal region, this technique is predictable for all types of ridge defects and can be used for routine patients.

FINANCIAL DISCLOSURE

This work is not supported by any financial assistance.

CONFLICT OF INTEREST

The authors declare that they have no conflicts of interest.

REFERENCES

[1] Seibert JS. [1983] Reconstruction of deformed partially edentulous ridges, using full thickness onlay grafts. Part I Technique and wound healing. *Compend Cont Ed Gen Dent* 4; 437–453

[2] Dahlin C, LindheA, Gottlow J, Nyman S. [1988] healing of bone defects by guided tissue regeneration. *Plast Reconstr Surgery* 81:672–673.

[3] Bruser D, Bragger U, Lang N, Nyman S. [1990] Regeneration and enlargement of jaw bone using guided bone regeneration. *Clin Oral Implants Res* 1:22–32.

[4] Seibert J, Nyman S. [1990] Localized ridge augmentation in dogs. A pilot study using membranes and hydroxyapatite. *J Periodontol* 61:157–165.

[5] Nevins M, Melloning J. [1992] Enhancement of the damaged edentulous ridge to receive dental implants: A combination of allograft and Gore-Tex membrane. *Int J Periodontics Restorative Dent* 12: 96–111.

[6] Buser D, Dula k, Belser U, Hirt HP, Barthold H. [1993] Localized ridge augmentation using guided bone regeneration. 1. Surgical procedure in the maxilla. *Int J Periodontics Restorative Dent* 13: 29–45.

[7] Wennstrom J. Mucogingival therapy. [1996] *Ann Periodontal* 1:671–701.

[8] Allen E, Gainza C, Farthing G, Newbold D. [1985] Improved technique for localized ridge augmentation a report of 24 cases. *J Periodontol* 56:195–199.

[9] Gray J, Quattlebaum J. [1988] Correction of localized alveolar ridge defects utilizing hydroxyapetite and a "tunneling" approach: A case report. *Int J Periodontics Restorative Dent* 8(3): 73–78.

[10] Siebert J, Salama H. [1996] Alveolarridge preservation and reconstruction. *Periodontol* 2000 11:69–84

[11] Gasparini D Orlando. [2004] Double fold connective tissue Pedicle Graft: A Novel Approach for ridge augmentation: *Int J Periodontics Rest dent* 24; 280–287.

[12] Abrams L. [1980] Augmentation of the deformed edentulous ridge for fixed prosthesis. *Compend Contin Educ Dent* 1:205–214.

[13] Scharf D, Tarnow D. [1992] Modified roll technique for localized ridge augmentation. *Int J Periodontics Rest dent* 12:415–425.

[14] Studer SP, Naef R, Schatet P. adjustment of localized alveolar ridge defects by soft tissue transplantation to improve mucogingival esthetics: a proposal for clinical classification and an evaluation of procedures.

[15] Orth CHF. [1996]. A modification of the connective tissue graft procedure for the treatment of type II and type III ridge deformities. *Int J Periodontics Restorative Dent* 16:267–277.

ISSN: 0976-3104
REGULAR ISSUE
Mushtaq et al.

THE IIOAB JOURNAL

RESEARCH ARTICLE OPEN ACCESS

INHIBITORY EFFECTS OF TIMOLOL MALEATE AND ITS PRESERVATIVE BENZALKONIUM CHLORIDE ON CORNEAL EPITHELIAL MIGRATION IN A RABBIT ORGAN CULTURE SYSTEM

Shamin Mushtaq [1, 2], Anwar Ali Siddiqui[3], Nikhat Ahmed[1*]

[1]*Neurochemistry Research Unit, Department of Biochemistry, University of Karachi, PAKISTAN*
[2]*National Center for Proteomics, University of Karachi,* [3]*Department of Biological and Biomedical Sciences, Aga Khan University, Karachi, PAKISTAN*

ABSTRACT

Purpose: *Timolol maleate, the ophthalmic solutions, is frequently prescribed for glaucoma, although the use of this drop is likely to interfere with wound healing in corneal surgeries. A possible factor that may influence rates of corneal wound healing is how the solutions are preserved. The purpose of this study to evaluate the effect of commercially prepared topical timolol maleate and its preservative benzalkonium chloride (BAC-) 0.0004% and 0.001% or its preservative free effect on the rate of corneal epithelial wound healing.* ***Methods:*** *In this study, New Zealand white rabbits corneas (n= 80) were removed and 7mm epithelia were abraded mechanically. The abraded corneal epithelia were incubated in modified supplemental hormonal epithelial media (SHEM) containing a) timolol maleate drop 0.005% and 0.05% supplied with BAC+ (0.001%) and b) BAC- (preservative free) timolol maleate (purified form) 0.005% and 0.05% and c) along with BAC+ 0.001% and 0.0004% concentration, d) only BAC with 0.001% and 0.0004% concentration. The media containing timolol maleate and BAC was replaced every 24 hours. Photographic documentation of Richardson stained, non-healed areas, was performed at time points 0, 24, 48, 72, 96 and 120 hours of post wounding.* ***Results:*** *The timolol maleate (0.05%) BAC accelerated wound healing and wound closure significantly ($p<0.001$), compared to controls. Delayed wound healing and wound closure at 120 hours was demonstrated only by timolol maleate drop at both concentrations (0.005% and 0.05%). Corneas treated only with BAC (0.001%) demonstrated delayed healing and wound closure was observed at 120 hours of post wounding. However, timolol maleate with relatively low concentration of BAC 0.0004% did not show any significant effect on wound healing ($p<0.05$).* ***Conclusion:*** *Corneal organ culture model has confirmed that topically applied timolol maleate inhibited corneal wound healing with its preservative BAC, although the appropriate randomized clinical assessment are essential to certify these reports.*

Received on: 16th -Sept-2011
Revised on: 4th-Dec-2011
Accepted on: 4th– Dec-2011
Published on: 10th –Feb -2012

KEY WORDS

Timolol maleate; benzalkonium chloride,cornea; wound healing

***Corresponding author:** Email: nikhat_ahmed14@yahoo.co.uk, alishamim99@yahoo.com; Tel: +92-21-9261300 Ext: 2346; Fax: 92-21-9261340

[I] INTRODUCTION

Beta blockers eye drops contain preservative to prevent contamination during the treatment period of the patient. Preservatives for ophthalmic solutions include benzalkonium chloride (BAC), chlorobutanol, parahydroxybenzoates and polysorbate.

Timolol maleate has been the drug of choice in the treatment of ocular hypertension and associated glaucoma for over two decades [1-3]. Drug related complications including chronic systemic and ocular side effects as a result of prolonged usage are a major concern [4-8]. Among the ocular side effects, corneal re-epithelialization remains a debatable issue. While some studies have reported β-blockers to significantly delay corneal epithelial wound healing [9-11], others strongly suggest non-deleterious effects on this phenomenon [12, 13].

One of the leading factors attributed to impaired wound healing following β-blocker administration is the presence of benzalkonium chloride (BAC), a preservative used in almost all β-blocker eye drop preparations. Numerous reports describe the preservative cytotoxicity which has been investigated extensively [16-18] and have revealed BAC to cause a delay in wound closure [14-16]. However it has been documented that

THE IIOAB JOURNAL
ISSN: 0976-3104

BAC alone does not appear to exert any effect on corneal epithelial wound healing [12].

The first evidence to a biological function for beta blocker in wound healing came from an early study indicating that beta blocker delayed skin wound healing in newt limbs [19]. However subsequent studies in other epithelia yielded conflicting results. For example, it has been reported that beta blocker either delay [10, 20] or enhance [12] corneal epithelial wound healing.

On account of the disparity in reported literature, a series of experiments have been designed for a better understanding of the extent of contribution of the commercially available β-blocker eye drop, timolol maleate and its preservative, BAC, and thereby, abet in the development of a safer therapeutic composition of the drug. Thus, our work uncovers the effects of timolol maleate, a commonly prescribed ophthalmic preparation, on corneal epithelial wound healing following buffering of the effects of BAC. Clearly, further investigation will improve our understanding of the corneal wound healing and hopefully escort to the development of new therapies to enhance wound healing.

[II] MATERIALS AND METHODS

2.1. Animals

New Zealand white rabbits (n= 40) weighing 2-3 kg used in this study was in conformity to the Declaration of Helsinki on the "Guiding Principle in Care and Use of Animals". Fresh eyes were obtained from a University slaughter house within 30 minutes following decapitation.

2.2. Wound Model

Rabbit corneal epithelial organ cultures were prepared as described previously [21, 22]. The Albino rabbit eyes were used to prepare migrating (n=60) and nonmigrating (n=20) corneal epithelia in organ culture. Four sets of experiment were performed in triplicates. The integrity of the corneas was checked with fluorescein. Rabbits with intact corneas were decapitated and their eyes processed immediately on ice. Following three washes in saline, the corneas were demarcated with a 7 mm trephine, and the epithelium within this region was subsequently removed with a scalpel blade (#10) under a dissecting microscope (Olympus M081). The corneas were then excised along 1-3 mm scleral rim, for non-migrating epithelium, excised similarly without scraping the epithelium and rinsed in Hanks Balanced Salt Solution (HBSS) (Sigma, St.Louis, MO) and disinfected for 5-7 minutes in antibiotic-antimycotic solution. The corneas were again rinsed in HBSS and transferred to modified Supplemental Hormonal Epithelial Media (SHEM) [24] containing fetal calf serum (5 %). The cultures were then incubated at 37 °C in a CO_2 incubator; media was replaced every 24 hours. The media containing beta blocker (timolol maleate)/or and BAC was also similarly processed.

2.3. Treatment Groups

The rabbit eyes were randomly assigned to one of four treatment group; each group consisted of twenty eyes. One group served as SHEM treated control. Timolol maleate and its trade names and manufacturers, vehicle, Benzalkonium chloride (BAC) are given in **Table– 1**.

2.4. Drugs

Commercially available timolol maleate eye drop (0.5% Remington) was used with 0.05% and 0.005% concentrations. Preservative BAC free (BAC-) timolol maleate (purified form, Sigma-Aldrich) was also prepared with concentrations, similar to eye drop, 0.05% and 0.005% and (BAC-) (0.001% and 0.0004%). Timolol maleate and BAC were dissolved directly in SHEM medium to give the desired concentrations.

Table: 1. Timolol Maleate and BAC Treatment

Group	Treatment	Con. (%)	Trade Name
1	SHEM (Control)	-	Sigma Aldrich
2	Timolol Maleate (D)	0.005	Remington Pharmaceutical
	Timolol Maleate (P) BAC-	0.005	Sigma Aldrich
	Timolol Maleate (P) BAC+ Timolol Maleate (P) BAC+	0.005+0.0004% 0.005+0.001	Sigma Aldrich
3	Timolol Maleate (D)	0.05	Remington Pharmaceutical
	Timolol Maleate (P)BAC-	0.05	Sigma Aldrich
	Timolol Maleate (P) BAC+ Timolol Maleate (P) BAC+	0.05+0.0004% 0.05+0.001	Sigma Aldrich
4	BAC	0.0004% 0.001%	Sigma Aldrich

2.5. Wound analysis

At 0, 24, 48, 72, 96 and 120 hours every cornea in each group was Richardson stained and its size with remaining epithelium defect was measured and photographed. For the statistical analysis, a one way ANOVA was applied. The results were presented as mean ± SD and a value of $p<0.05$ is considered to be statistically significant.

[III] RESULTS

Corneas treated with the beta blocker timolol maleate in its drop and preservative free form along with BAC 0.001% showed delayed healing whereas timolol maleate with 0.0004% BAC did not show any significant delay. However, in corneas treated with SHEM (control) wound closure occurred at 72 hour of post wounding. A comparison of data obtained on the corneal epithelial wound healing (48 hours, which is the active phase of migration) rates of all organ culture preparations is summarized in **Table–2**. At 24 hours there was no difference in the wound healing rates among all the treated corneas.

THE IIOAB JOURNAL
ISSN: 0976-3104

Table. 2: Rate of Corneal Epithelial Wound Healing at 48 Hours of Post Wounding.

Treatment	Con (%)	Number of eyes	Rate of Healing at 48 hours (mm^2/hr±SEM)	P-value compared with SHEM treated control	Time for wound closure (hours)
SHEM	-	6	0.61 ± 0.98	-	72
Timolol Maleate (D)	0.005	6 each	0.53 ± 1.88	P<0.001	120
Timolol maleate (P) BAC-	0.005		0.58 ± 1.24		72
Timolol Maleate (P) BAC+	0.0004		0.56 ± 1.46		72
Timolol Maleate (P) BAC+	0.001		0.55 ± 1.57		96
Timolol Maleate (D)	0.05	6 each	0.50 ± 0.52		120
Timolol Maleate (P) BAC-	0.05		0.58 ± 0.10		72
Timolol Maleate (P) BAC+	0.0004		0.57 ± 1.47	P<0.001	72
Timolol Maleate (P) BAC+	0.001		0.52 ± 1.47		96
BAC only	0.0004 0.001		0.59 ± 0.99 0.48 ± 1.77	P<0.05	96 120

The corneas treated with beta blocker timolol maleate drop (Remington) 0.005% which contained BAC (0.001%) showed wound closure at 120 hours. Whereas at the same concentration of timolol maleate preservative free BAC- group of corneas showed wound closure at 72 hour. We observed a delay in wound healing and subsequent wound closure at 96 hours ($p< 0.001$) in corneas treated with a combination of 0.001% BAC with 0.005% timolol maleate , whereas 0.0004% BAC with 0.005% timolol maleate did not show any significant difference **[Figure– 1]**.

Corneas treated with timolol maleate drop 0.05% **[Figure– 2]** and its preservative free form showed wound closure at 120 and 72 hours respectively whereas 0.0004% BAC with 0.05% timolol maleate revealed no significant effect on the rate of healing. Timolol maleate with 0.001% BAC took longer time to heal and the wound closure occurred at 96 hours of post wounding ($p<0.001$). Similarly only BAC 0.001% treated corneas showed delayed wound closure compared to the control and it also profoundly impedes wound closure at 120 hours **[Figure– 3]**. However, we observed facilitated wound healing in corneas treated with 0.0004% BAC alone ($p<0.05$) following wound closure at 96 hours **[Figure– 4 A, B, C]**.

[IV] DISCUSSION

Corneal epithelial wound healing following exposure to varying concentrations of the tested commercial ophthalmic solutions timolol maleate was prompted in the absence of preservative (BAC).

Numerous reports described the toxic effect of beta blockers along with their preservative, BAC, disparity in peer-reviewed literature demand more extensive studies to better understand the contribution of each in corneal toxicity [2, 3, 19].

The present study was conducted to investigate the extent of inhibitory effect on corneal epithelial wound healing induced by the commercially available β-blocker, Timolol maleate, following buffering of the effects of its preservative, BAC. These effects on ocular surface tissue may be caused in part by preservatives usually applied with the therapeutic agent [25].

Corneal epithelial healing rates in response to an abrasion in organ cultures were carried out, which is a well established experimental means of evaluating corneal toxicity [26]. In the present organ culture model we considered it appropriate to determine the optimum concentration of BAC at which the rate of healing was similar to that of the untreated controls. This

THE IIOAB JOURNAL
ISSN: 0976-3104

buffering effect was found to occur at a concentration of 0.001% of BAC. On the contrary the same concentration of preservative (0.001%) in the presence of two different concentrations of Timolol maleate, (0.005% and 0.05%) induced a delay in the wound healing rate. Our observations are consistent with a number of studies that have reported β–blockers to inhibit corneal re-epithelialization [10, 11] and BAC to significantly retard wound healing upon prolonged use [10]. Trope et al [9] showed Betagan treated corneas to induce mild superficial epithelial changes with loss of microvilli or slight desquamation.

It is noteworthy that levobunolol, the β–blocker by itself has shown little effect on the corneal epithelial surface [13] and additionally enhanced the rate of wound healing [12]. Interestingly, BAC, which was found to disrupt the integrity of the outermost corneal epithelial layers, enhanced the transcorneal levobunolol flux and reduced its extent of metabolism [26]. This may provide an explanation for the combined toxic effect of BAC and levobunolol.

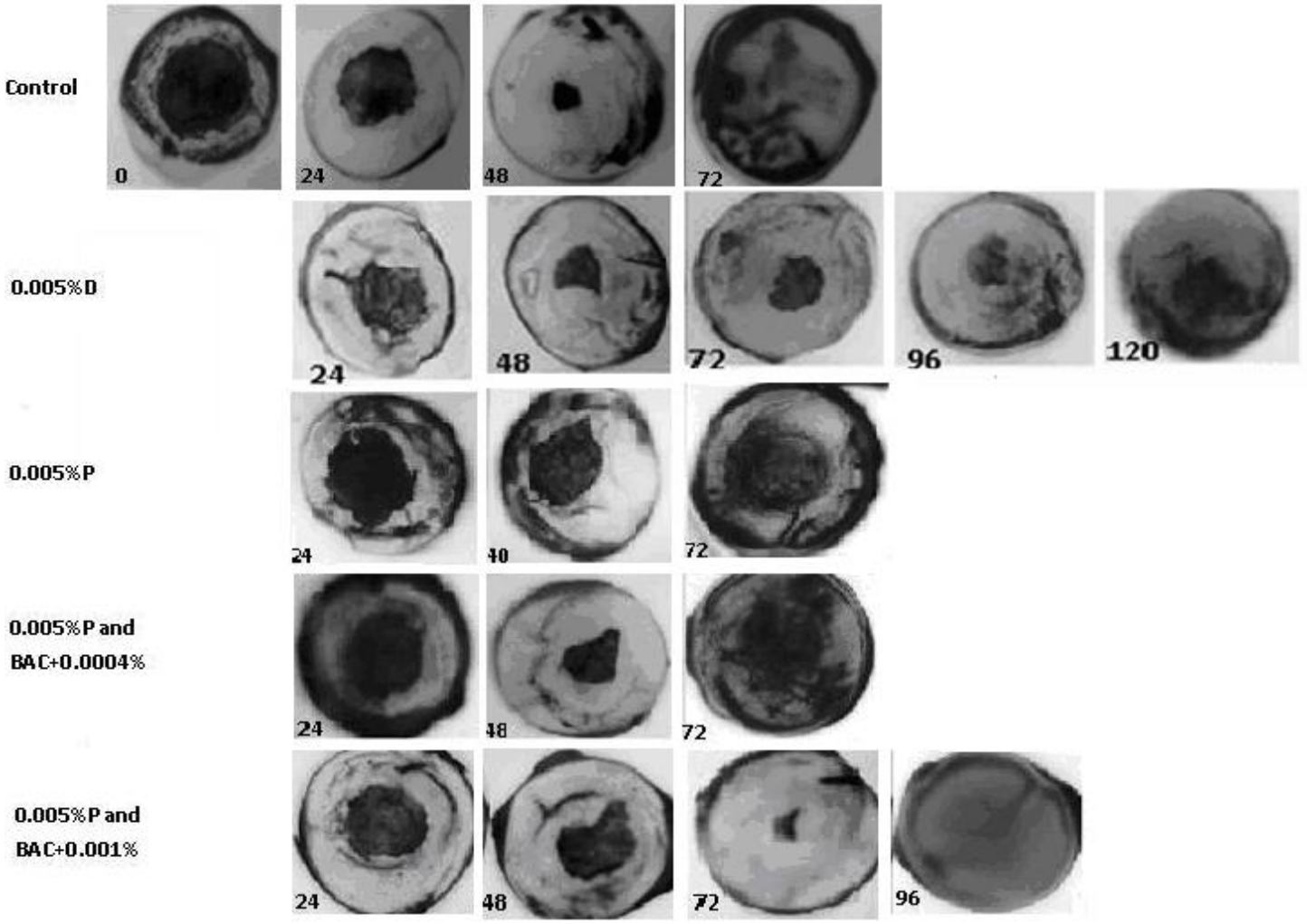

Fig. 1: Corneal epithelia treated with timolol maleate (Drop 0.005% and BAC- 0.005% with combination of BAC+ 0.0004% and 0.001% concentration. Wound healing was observed at different time interval represents 24, 48, 72, 96 and 120 hours. Scraped cornea after harvesting of epithelium 0 hour, arrows indicates 7 mm scraped region. At 72 hours, complete wound closure occurred at this time point in control. Corneas visualized with Richardson stain show the migrating epithelial cell from the wound margin to the center of wound.

THE IIOAB JOURNAL
ISSN: 0976-3104

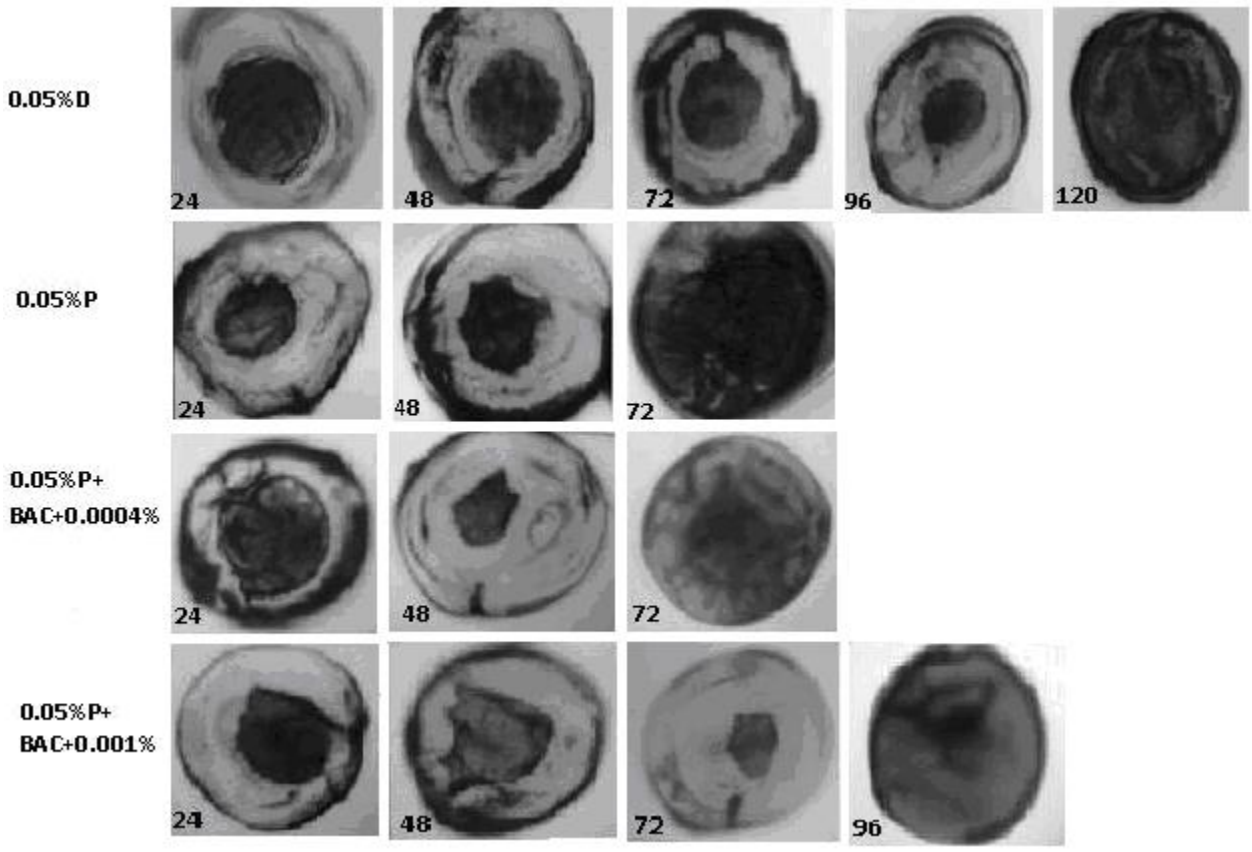

Fig. 2: Corneal epithelia treated with timolol maleate (Drop 0.05% and BAC- 0.05% with combination of BAC+ 0.0004% and 0.001% concentration. Wound healing was observed at different time interval represents 24, 48, 72, 96 and 120 hours. At 72 hours, complete wound closure occurred at this time point in control. Corneas visualized with Richardson stain show the migrating epithelial cell from the wound margin to the center of wound.

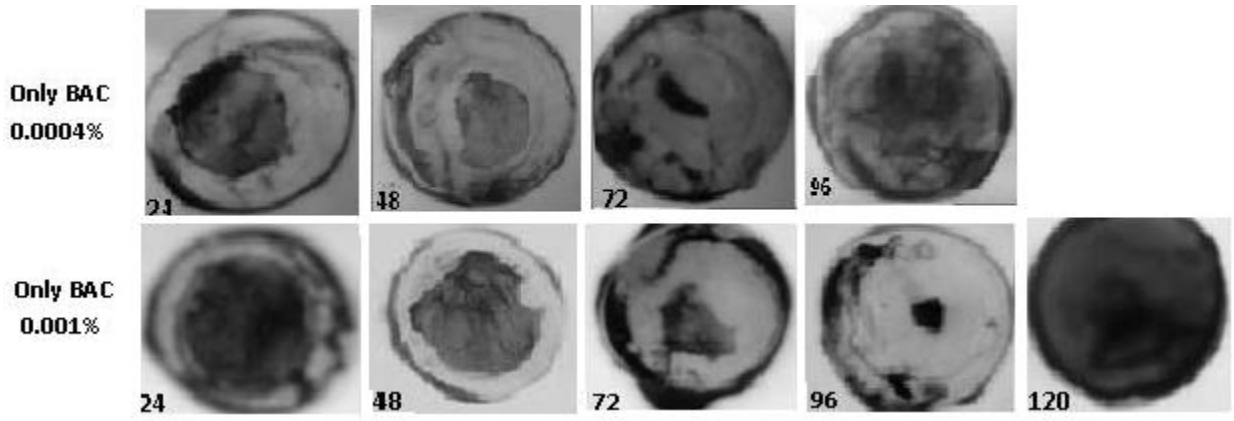

Fig. 3: Corneal epithelia treated with only BAC 0.0004% and 0.001% were analyzed for wound healing at different time interval represents 24, 48, 72, 96 and 120 hours of post wounding. Corneas visualized with Richardson stain show the migrating epithelial cell from the wound margin to the center of wound.

THE IIOAB JOURNAL
ISSN: 0976-3104

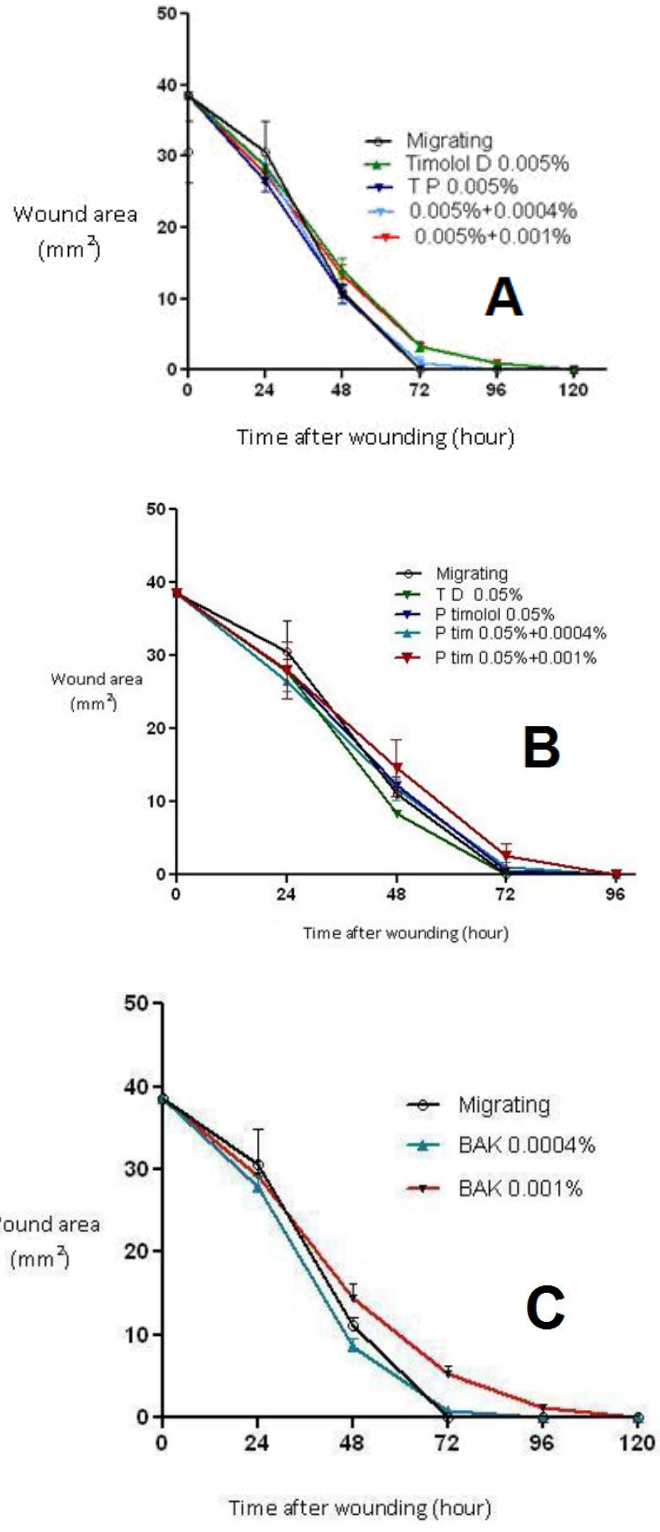

Fig. 4: In vitro wound healing of timolol maleate treated corneal epithelia with (A) drop 0.005%, BAC- and BAC+ 0.0004% and 0.001%. (B) Timolol maleate 0.05% BAC- and BAC+ 0.0004% and 0.001% concentrations (C) only BAC 0.0004% and 0.001% with control (without treatment) normal migrating corneal epithelia in organ culture. This shows average epithelial wound area at 24, 48 and 72 hours after wounding. The figure shows the phases of wound healing 0-24, 24-48, 48-72, 72-96 and 96-120 hours. Time to complete wound closure is seen at 72 hours in control group (without treatment). Each value represents six corneas and error bar indicates SEM.

This study convincingly indicates that following buffering of the adverse effects of BAC, timolol maleate remains a potential hazard for the corneal wound healing. The BAC, which is used as a preservative in almost all beta-blockers, has shown inhibition in the rate of healing of the corneas **[Figure– 4 A, B, C]**. In the light of our results it is doubtful whether the concentrations to which the corneal epithelium is exposed to beta blockers (containing preservative) after surgeries in the common clinical therapeutics doses should be continued. Further investigations of individual components of beta blockers are necessary to fully understand ophthalmic solution cytotoxicity

FINANCIAL DISCLOSURE

This work is not supported by any grant.

CONFLICTS OF INTERESTS

The authors declare no conflicts of interest.

REFERENCES

[1] Tan AY, LeVatte TL, Archibald ML, et al. [2002] Timolol concentrations in rat ocular tissues and plasma after topical and intraperitoneal dosing. *J Glaucoma* 11:134-142.
[2] Zimmerman TJ. [1993] Topical ophthalmic β-blockers: a comparative review. *J Ocul Pharmacol* 9:373–384.
[3] Zimmerman TJ and Kaufman HE. [1977] Timolol: A □-adrenergic blocking agent for the treatment of glaucoma. *Arch Ophthalmol* 95: 601–604.
[4] Everitte DE and Avoron J. [1990] Systemic effects on medications used to treat glaucoma. *Ann Intern Med* 112: 120–150.
[5] Ohtsuki M, Yokoi N, Mori K, et al. [2001] Adverse effects of β-blocker eye drops on the ocular surface. *Nippon Ganka Gakkai Zasshi*; 105:149–154.
[6] Koraszewska-Matuszewska B. [1999] Pharmacotherapy of congenital glaucoma in young children. *Klin Oczna* 101:393–396.
[7] Thygesen J, Aaen K, Theodorsen F, et al. [2000] Short-term effect of latanoprost and timolol eye drops on tear fluid and the ocular surface in patients with primary open-angle glaucoma and ocular hypertension. *Acta Ophthalmol Scand* 78:37–44.
[8] Herreras JM, Pastor JC, Calonge M, Ansensio VM. [1992] Ocular surface alteration after long-term treatment with an antiglaucomatous drug. *Ophthalmology* 99: 1082–1088.

THE IIOAB JOURNAL
ISSN: 0976-3104

[9] Trope GE, Liu GS, and Basu PK. [1998] Toxic effects of topically administered Betagan, Betoptic, and Timoptic on regenerating corneal epithelium. *J Ocul Pharmacol* 4:359–366.

[10] Haruta Y, Ohashi Y, and Matsuda S. [1997] Corneal epithelial deficiency induced by the use of β-blocker eye drops. *Eur J Ophthalmol* 7:334–339.

[11] Liu GS, Trope GE, Basu PK. [1990] β -adrenoceptors and regenerating corneal epithelium. *J Ocul Pharmacol* 6:101–112.

[12] Reidy JJ, Zarzour J, Thompson HW, Beuerman RW. [1994] Effect of topical β -blockers on corneal epithelial wound healing in the rabbit. Br J Ophthalmol 78:377–380.

[13] Follmann P, Varga M, Daroczy J. [1989] The effect of timolol, betaxolol and levobunolol on the surface of rabbit cornea. *Int Ophthalmol* 13:81–84.

[14] Tripathi BJ, Tripathi RC, Koli SP. [1992] Cytotoxicity of Ophthalmic preservatives on human corneal epithelium. *Lens Eye Tox Res* 9:361–375.

[15] Kossendrup D, Wiederholt M, Hoffmann F. [1986] Influence of cyclosporin A, dexamethasone, and benzalkonium chloride on corneal epithelial wound healing in the rabbit and guinea pig eye. *Cornea* 4:177–181.

[16] Collin HB, Grabsch BE. [1982] The effect of ophthalmic preservatives on the healing rate of the rabbit corneal epithelium after keratectomy. *Am J Optom Physiol Opt* 59:215–222.

[17] D'Angelo G, Lambiase A, Cortes M, et al. [2003] Preservative-free diclofenac sodium 0.1% for vernal keratoconjunctivitis. Graefe's. *Arch Clin Exp Ophthalmol* 241: 192–195.

[18] Green K, Johnson RE, Chapman JM, et al. [1989] Preservative effects on the healing rate of rabbit corneal epithelium. *Lens Eye Toxic Res* 6:37–41.

[19] Donaldson DJ, Mahan JT. [1984] Influence of catecholamines on epidermal cell migration during wound closure in adult newts. Comp *Biochem Physiol C*. 78: 267–270.

[20] Liu GS, Trope GE, Basu PK. [1990] Beta adrenoceptors and regenerating corneal epithelium. *J Ocul Pharmacol* 6: 101–112.

[21] Mushtaq S, Naqvi ZA, Siddiqui AA, et al. [2007] Changes in albumin precursor and heat shock protein 70 expression and their potential role in response to corneal epithelial wound repair. *Proteomics* 7: 463–468.

[22] Mushtaq S, Zulfiqar A Naqvi, Anwar A. Siddiqui, and Nikhat Ahmed. [2007] Albumin Precursor and Hsp70 modulate corneal wound healing in an organ culture model. *Acta Histochemica* 113(1):36–42.

[23] Zieske JD, Gipson IK. [1986] Protein synthesis during corneal epithelial wound healing. *Invest Ophthalmol Vis Sci* 27: 1–7.

[24] Tan AY, LeVatte TL, Archibald ML, et al. [2002] Timolol concentrations in rat ocular tissues and plasma after topical and intraperitoneal dosing. *J Glaucoma* 11:134–142.

[25] Crossen CE, Klyce SD, Beuerman RW. [1986] Epithelial wound closure in the rabbit cornea: a biphasic phase. *Invest Ophthalmol Vis Sci* 27:464–473.

[26] Ashton P, Wang W, Lee VH. [1991] Location of penetration and metabolic barriers to levobunolol in the corneal epithelium of the pigmented rabbit. *J Pharmacol Exp Ther* 259:719–724.

ISSN: 0976-3104

REGULAR ISSUE
Rajasekaran and kalaivni.

RESEARCH ARTICLE OPEN ACCESS

ANTIOXIDANT ACTIVITY OF AQUEOUS EXTRACT OF MONASCUS FERMENTED INDIAN VARIETY OF RICE IN HIGH CHOLESTEROL DIET FED-STREPTOZOTOCIN DIABETIC RATS, AN IN VIVO STUDY

Rajasekaran A, Kalaivani M*.

KMCH College of Pharmacy, Coimbatore, Tamil Nadu, INDIA

ABSTRACT

Objective: *The present study was designed to investigate antioxidant activity of aqueous extract of Monascus fermented Indian variety of rice in high cholesterol diet fed- streptozotocin induced diabetic rats.* ***Methods:*** *The Indian variety rice IR-532-E-576 was fermented with Monascus purpureus for 10 days. After 10 days of fermentation it was sterilized by autoclaving and extracted with boiling water. High cholesterol fed- streptozotocin-induced diabetic rats were administered with aqueous extract of Monascus fermented Indian variety of rice at the concentration of 1.2 g / Kg of bw and 2.4 g / Kg bw daily for 30 days. The oxidative parameters like lipid peroxidation, reduced glutathione, superoxide dismutase and catalase activities were assessed.* ***Results:*** *Administration of high cholesterol diet and streptozotocin to experimental animals showed significant ($p<0.001$) increase in the level of lipid peroxidation and significant ($p<0.001$) reduction in the level of superoxide dismutase, reduced glutathione and catalase, whereas on administration of aqueous extract of Monascus purpureus fermented Indian variety of rice reduced the level of lipid peroxidation to almost normal, significantly ($p<0.05$) and increased the levels of reduced glutathione, superoxide dismutase and catalase, significantly ($p<0.05$) at the dose of 1.2 g / Kg of bw and 2.4 g / Kg bw.* ***Conclusion:*** *Diabetes mellitus and hyperlipidemia leads to oxidative stress, from the present study it was concluded that consumption of Monascus fermented rice, having antioxidant activity in vivo can be good dietary supplement for diabetes induced hyperlipidemia. Antioxidant benefits of Monascus fermented rice can be utilized in reducing the risks due to oxidative stress.*

Received on: 9th-Sept -2010
Revised on: 27th-Feb-2011
Accepted on: 15th–Mar-2011
Published on: 15th–Feb–2012

KEY WORDS

Monascus; fermentation; diabetic; anti-oxidant

Corresponding author: Email: kala_samy2002@yahoo.com; Tel: +91-452-2458478; Fax: +91-452-2459873

[I] INTRODUCTION

Oxidative stress has been one of the important mechanisms for molecular and cellular damage of tissue. Oxygenated compounds, especially aldehydes such as melondialdehyde (MDA) and conjugated dienes, are produced during the attack of free radicals to membrane lipoproteins and polyunsaturated fatty acids. Thus oxidative stress plays an important role in the process of aging and pathogenesis of numerous diseases like diabetes, cancer, neurodegenerative diseases, and respiratory tract disorders [1]. Diabetes mellitus is a chronic metabolic disorder characterized by a high blood glucose level due to insulin deficiency, often combined with insulin resistance [2]. Diabetes mellitus leads to abnormalities in carbohydrate and lipid metabolism which results in excessive production of reactive oxygen species and oxidative stress [3, 4, 5, 6, 7]. Hyperlipidemia is the presence of raised or abnormal levels of lipids and/or lipoproteins in the blood. According to latest studies hyperlipidemia leads to oxidative stress [8]. Enzymic antioxidants like superoxide dismutase and glutathione peroxidase and non-enzymatic antioxidants play an important role in preventing the tissue damage due to the formation of free radicals. Usage of antioxidants helps in reducing risks of oxidative damages in diabetic and hyperlipidemic patients [9, 10]. Red yeast rice (RYR) is a fermented rice product produced traditionally by fermenting cooked rice kernels with yeast Monascus sp. The use of red yeast rice in China dates back to first century. RYR was mentioned in ancient Chinese pharmacopoeia of medicinal food and herbs, where it is given as a medicine for digestion and revitalization [11]. It contains six pigments and other metabolic products from Monascus sp., such as alcohols, organic acids, and substances with a wide range of biological and therapeutic benefits, including anti-carcinogenic, anti-oxidative, and hypolipidemic activities [12]. As both diabetes mellitus and hyperlipidemia leads to oxidative stress, antioxidant benefits of RYR can be utilized in reducing the risks due to oxidative stress. In our present work antioxidant property of Monascus fermented Indian variety of rice was studied in diabetes -induced high cholesterol fed rats.

THE IIOAB JOURNAL
ISSN: 0976-3104

[II] MATERIALS AND METHODS

Materials

Streptozotocin (STZ) and all other chemicals used for this study were purchased from Sigma, USA. Indian variety of rice from local market, Coimbatore, Tamil Nadu.

2.1. Production of Monascus fermented rice

Monascus fermented rice was produced by solid state fermentation of Indian variety of rice with Monascus purpureus at the concentration of 107 spores/ mL for 10 days at 30°C. Fungal culture of Monascus purpureus MTCC 1090 was obtained from The Institute of Microbial technology, Chandigarh, India.

2.2. Preparation of Monascus fermented rice extract

The dried Monascus purpureus fermented Indian rice was crushed and used for extraction with water by boiling at 100°C for 4 hours. Extract was filtered and used for further studies [13, 14].

2.3. Evaluation of anti-oxidant activity

2.3.1. Experimental animal model

Male Wistar Albino rats weighing 200-250g were used in the present study. All rats were kept at room temperature of 22°C in the animal house. All animal procedures were performed after approval from the institutional animal ethical committee of Kovai Medical Centre Research and Educational Trust, Coimbatore, Tamil Nadu, India (Approval no:KMCRET/Ph.D/1/2009). All animals were maintained in accordance with the internationally accepted ethical guidelines for the care of laboratory animals. Prior to the experiments, rats were fed with standard food for one week in order to adapt to the laboratory conditions.

2.4. Induction of diabetes

Diabetes was induced in overnight fasted adult Wistar Albino rats weighing 200-250g by single intra-peritoneal(i.p) injection of 60 mg/kg of STZ dissolved in citrate buffer (pH 4.5). Hyperglycemia was confirmed by elevated glucose levels in plasma, determined at 72 hour and then on day 7 after injection. The threshold value of fasting plasma glucose to diagnose diabetes was taken as >126mg/dL.Only rats found with permanent diabetes (except for control group) were selected for the antioxidant study and are fed with high cholesterol diet (2% w/v cholesterol with standard pellet diet).

2.5. Experimental design

Thirty animals were divided into five groups, each consisting of six animals. Group 1 animals were non-diabetes induced, received normal diet (Control group).Group 2 animals were diabetes induced fed with high cholesterol diet and received oral administration of 2 mL of sterile water. Group 3 and 4 were diabetes induced, fed with high cholesterol diet and received oral administration of Monascus fermented rice extract at the dose of 1.2 and 2.4 mg/kg bw (body weight) respectively in 2 mL of sterile water for 30 days. Group 5 was diabetic induced and fed with high cholesterol diet and received oral administration of reference hypoglycemic drug with antioxidant activity gilbenclamide 10 mg/kg bw in 2 mL of sterile water for 30 days. In group 2, 3, 4 and 5 diabetes was induced by administration of STZ at dose 60mg/kg bw, i.p.

2.6. In vivo antioxidant activity

2.6.1. Preparation of tissue homogenate

The tissues were weighed and 10% w/v tissue homogenate was prepared by mincing and homogenizing the tissues in 0.1 M phosphate buffer (pH 7.5). After centrifugation at 10,000 rpm for 10 minutes, the clear supernatant was used for the estimation of non-enzymatic and enzymatic antioxidants.

2.7. Estimation of lipid peroxidation (LPO) in liver tissue

Lipid peroxidation in liver tissue was estimated colorimetrically by TBARS and hydroperoxides. 0.1 mL of tissue homogenate in Tris-HCl buffer (pH 7.5) was treated with 2 mL of TBA-TCA-HCl reagent (TBA 0.37%, 0.25N HCl and 15% TCA-1:1:1 ratio) and placed in water bath for 15 min and cooled. The absorbance of clear supernatant was measured against reference blank at 535nm spectrophotometrically. The lipid peroxidation was calculated on the basis of the molar extinction coefficient of MDA and expressed as nm MDA/g protein [15, 16].

Estimation superoxide dismutase (SOD) in liver tissue

The activity of SOD was assayed by the method of Kakkar et al [17]. 0.5 mL of tissue homogenate was diluted with 1mL of water. To this mixture, 2.5 mL of ethanol and 1.5 mL of chloroform (all reagents chilled) were added and shaken for 1 min at 4°C and then centrifuged. The supernatant was taken. The assay mixture containing 1.2 mL of sodium pyrophosphate buffer (0.025 M, pH 8.3), 0.1ml of 186 µM PMS, 0.3 mL of 30 µM NBT, 0.2 mL of 780 µM NADH, appropriately diluted enzyme preparation and water in a total volume of 3 mL. Reaction was started by the addition of NADH. After incubation at 30°C for 90 seconds the reaction was stopped by the addition of 1mL glacial acetic acid. The reaction mixture was stirred vigorously and shaken with 4mL of n-butanol. The intensity of the chromogen in the butanol layer was measured at 560nm against butanol blank. Assay mixture devoid of enzyme served as control. One unit of the enzyme activity is defined as the enzyme reaction, which gave 50% inhibition of NBT reduction in one minute under the assay conditions.

Estimation of reduced glutathione (GSH) in liver tissue

GSH was determined by the method of Ellman (1959) [18]. 0.5mL of tissue homogenate was precipitated with 2mL of 5% TCA and centrifuged at 3200×g for 20 minutes. After centrifugation, 1mL of the supernatant was taken and added to 0.5mL of Ellman's reagent (2, 2´-dinitro-5, 5´-dithiobenzoic acid) and 3mL of phosphate buffer (pH 8.0). Then the absorbance was measured at 412nm.The values were expressed as mg/100 g tissue.

Estimation of catalase in liver tissue

The reaction mixture for the estimation of catalase activity contained 1.0 mL of 0.01M pH 7.0 phosphate buffer, 0.1 mL of tissue homogenate (supernatant) and 0.4 mL of 2M H_2O_2 in a total volume of 1.5 mL. The reaction was stopped by the addition of 2.0 ml of dichromate-acetic acid reagent (5% potassium dichromate and glacial acetic acid mixed in 1:3 ratio). Then the absorbance was measured colorimetrically at 620 nm and it is expressed as µmoles of H_2O_2 consumed/min/mg protein as described by Sinha 1972 [19].

THE IIOAB JOURNAL
ISSN: 0976-3104

[III] RESULTS AND DISCUSSION

The results of antioxidant activity were showed in table 1. LPO, GSH, SOD and Catalase serve as markers in studying the antioxidant activity. Diabetes induced, high cholesterol fed rats showed 60% higher LPO when compared to the normal rats. Further SOD, GSH and Catalase were found to be decreased by 34, 97 and 33% respectively. The rats treated with Monascus fermented rice extracts at the concentration of 1.2 and 2.4 g/kg/day bw showed 33 and 31% reduction in LPO. The present study showed that the treatment with Monascus fermented Indian rice extract at the dose of 1.2 and 2.4 g/kg/day bw resulted in significant increase in GSH level to about 34 and 70% respectively. Antioxidant enzymes SOD and Catalase were also increased in their level to about 24 and 18% with supplementation of Monascus fermented Indian rice extract at the dose of 1.2 g/kg bw/day, respectively and about 34 and 33% at the dose of 2.4 g/kg bw/day, respectively.

STZ induces type 1 diabetes mellitus in the test animals resulting in hyperglycemia. High cholesterol diet leads to hyperlipidemia. Thus the test animals which are both hyperglycemic and hyperlipidemic are prone to the development of oxidative stress. The oxidative stress can be marked by LPO, GSH, SOD and Catalase levels. Oxidative stress results in increased LPO which plays an important role in several pathologies like atherosclerosis, diabetes, wound healing, liver disorder, inflammation etc [20]. The diabetes induced, high cholesterol fed animals showed increased LPO than in control animals.The animals treated with Monascus fermented rice extracts showed reduced LPO level when compared with untreated animals, which was better than the animals treated with standard drug (glibenclamide) [21]. GSH, SOD and Catalase protect the cell constituents from oxidative damage. Oxidative stress may lead to reduction in glutathione or inactivation of superoxide dismutase and catalase [22]. Concentration of these markers were found to be increased in animals treated with Monascus fermented Indian variety of rice extracts, which is also better than the standard drug glibenclamide. Thus the antioxidant activity of Monascus fermented Indian variety of rice was evident with the decreased LPO and increased SOD, GSH and Catalase in Monascus fermented Indian variety of rice extract treated rats.

ACKNOWLEDGEMENT

The authors acknowledge KMCH College of Pharmacy, Coimbatore, Tamil Nadu, India for providing instrumental support to carryout this research.

FINANCIAL DISCLOSURE

This work in not supported by any grant

CONFLICT OF INTERESTS

The authors declare no conflict of Interests

REFERENCES

[1] Anderson D, Phillips BJ, Tian-Wei YU, Edwards AJ, Ayesh R, Butterworth KR. [2000] Effects of vitamin C supplementation in human volunteers with a range of cholesterol levels on biomarkers of oxygen radical-generated damage. *Pure. Appl. Chem*. 72:973–983.

[2] Rang HP, Dale MM, Ritter JM, Flower RJ. [2003] In: Pharmacology. Elsevier Churchil Living stone, *New Delhi* 385–392.

[3] Ghiselli A, Laurenti O, De Mattia G, Maiani G, Ferro-Luzzi A. [I992] Salicylate hydroxylation as an early marker of invivo oxidative stress in diabetic patients. *Free Radical Biology and Medicine* 13:621–626.

[4] Gopaul NK, Anggard EE, Mallet AI, Betteridge DJ, Wolff SP, Nourooz Zadeh J. [1995] Plasma 8 epi-PGF2 alpha levels are elevated in individuals with non-insulin dependent diabetes mellitus.*FEBS Letter* 368:225–229.

[5] Nourooz Zadeh J, Tajaddini Sarmadi, Mc Carthy S, Beteridge DJ, Wolf SP. [1995] Elevated levels of authentic plasma hydroperoxides in NIDDM. *Diabetes* 44:1054–1058.

[6] Rehman A, Nourooz-Zadeh J, Moller W, Tritschler H, Pereira P, Halliwell B. [1999] Increased oxidative damage to all DNA bases in patients with type 2 diabetes mellitus. *FEBS Letter* 448:120–122.

[7] Shih PT, Elices MJ, Fang ZT, Ugarova TP, Strahl D,et al. [1999] Minimally modified low density lipoprotein induces monocyte adhesion to endothelial connecting segment by activating B1- integrin. *Journal of Clinical Investigation* 103: 613–625.

[8] Li Yang, Yong Hui Shi, Gang Hao, Wu Li, Guo-Wei Le. [2008] Increasing Oxidative Stress with Progressive Hyperlipidemia in Human: Relation between Malondialdehyde and Atherogenic Index. *J Clin Biochem. Nutr* 43:154–158.

[9] Minhajuddin M. [2005] Hypolipidemic and antioxidant properties of tocotrienol rich fraction isolated from rice bran oil in experimentally induced hyperlipidemic rats. *Food Chem Toxicol* 43:747–753.

[10] Yang R. [2006] Effect of antioxidant capacity on blood lipid metabolism and lipoprotein lipase activity of rats fed a high-fat diet. *Nutrition* 22:1185–1191.

[11] Heber D, Yip I, Ashley JM, Elashoff DA, Elashoff RM, Go VL. [1999] Cholesterol- lowering effects of a proprietary Chinese red yeast rice dietary supplement. *American Journal of Clinical Nutrition* 9:231–236.

[12] Ozlem Erdogul, Sebileazirak. [2004] Review of the studies on red yeast rice (Monasccus purpureus).Turkish electronic *journal of biotechnology* 2:37–49.

[13] Ricky WK, Bakr R. [2008] Chinese red yeast rice (Monascus pupureus fermented-rice) promotes bone formation. *Chinese Medicine* 3:4.

[14] Taeil Jeon, Seong Gu Hwang, Shizuka Hirai, Tohru Matsui, Hideo Yano,et al. [2004] Red yeast rice extracts suppress adipogenesis by down- regulating adipogenic transcription factors and gene expression in 3T3-L1 cells. *Life Sciences* 75: 3195–3203.

THE IIOAB JOURNAL
ISSN: 0976-3104

[15] Stocks J, Dormandy TL. [1971] Autooxidation of human red cell lipids induced by hydrogen peroxide. *Br J Hematol* 20: 95–111.

[16] Joharapurkar AA, Zambad SP, Wanjari MM, Umathe SN. [2003] In vivo evaluation of antioxidant activity of alcoholic extract of Rubia cordifolia linn. and its influence on ethanol-induced immunosuppression. *Indian Journal of Pharmacology* 35: 232–236.

[17] Kakkar P, Dos B, Viswnathan P. [1984] A modified spectrophotometric assay of superoxide dismutase. *Indian J Biochem* 21: 130–132.

[18] Ellman GL. [1959] Tissue sulfhydryl group. *Arch Biochem Biophys* 82: 70–77.

[19] Sinha AK. [1972] Colormetric assay of catalase. *Anal Bioche* 47:389–394.

[20] Karuna R, Reddy SS, Baskar R, Saralakumari D. [2009] Antioxidant potential of aqueous extract of Phyllanthus amarus in rats. *Indian J Pharmacol* 41:64–67.

[21] Elmali E, Atlan N, Bukan N. [2004] Effect of the sulphonylurea glibenclamide on liver and kidney antioxidant enzymes in streptozocin-induced diabetic rats. *Drugs RD* 5:203–208.

[22] Rai N, Maguchi S, Fugii S. [1997] Glycation and inactivation of human Cu-Zn-superoxide dimutase,identification of the in vitro glycated sites. *J.Boi.Chem* 262:16969–16972.

ISSN: 0976-3104
REGULAR ISSUE
Jovanov et al.

THE IIOAB JOURNAL

RESEARCH ARTICLE OPEN ACCESS

X- RAY DIFFRACTION AND MINERALOGICAL STUDY OF VERTISOL IN EASTERN MACEDONIA

Dalibor JOVANOV[1*], Tena SIJAKOVA-IVANOVA [2], Biljana PETKOVSKA[3]

[1] *Goce Delcev University, Faculty of Agriculture, Krste Misirkov b.b, 2000 Stip, MACEDONIA*
[2] *Goce Delcev University, Faculty of Natural and Technical Science, Goce Delcev 89, 2000 Stip, MACEDONIA*
[3] *Goce Delcev University, Faculty of Philology, Goce Delcev 89, 2000 Stip, MACEDONIA*

ABSTRACT

The paper is about mineralogy of vertisols spread out in Eastern Macedonia. Three basic soil profiles were selected to present the vertisols that occur in different parent materials (tertiary clay sediment, andesite tuff and andesite brecca).

X-ray diffraction (XRD) is known as the best method for the identification and quantification of minerals present in soil. This method is used in our research for determination of present minerals. The XRD results indicate that the main constituents of the coarser soil fractions (silt and sand) are quartz, feldspates and calcite, while in the profile developed on andesite breccia two very rare minerals were determined (Koashvite in hor. Aca is present with 81% and Winchinite in hor. C is present with 45.60%). In the finest clay fraction, montmorillonite and mixture-layer minerals (MLM) are dominant in all cases.

Received on: 40th-July -2011
Revised on: 20th-Oct-2011
Accepted on: 09th-Nov.-2011
Published on: 26th-Feb -2012

KEY WORDS

X-ray diffraction; clay minerals; koashvite; winchinite.

***Corresponding author:** Email: dalibor.jovanov@ugd.edu.mk ; Tel: +38-932-550-613

[I] INTRODUCTION

In Macedonia, the vertisol is spreading in about 61.900 ha. It is present mostly in the valleys and melioration areas (Stip, Probistip, Zletovo, Ovce Pole, Kumanovo, Skopje, Malesh and Pelagonia). Vertisols have high potential for the production of different food crops (wheat, maize, barley, garden-stuff, fodders, vine yards).

This type of soil is not much explored especially in the region of East Macedonia, as in physical and chemical characteristics, and in its mineralogy. In the coarser mineralogy fractions of vertislol there is a dominance of feldspate (usually 50-70%), and of quartz (20-30%) [1]. In the vertisols of Malesh and Kumanovo the montmoriilonite dominates in clay fraction [2]. There are similar results for the vertisols from Ghana, Congo, India, Morocco and Nigeria [3]. The dominance of montmorilonite in clay fractions is confirmed by numerous researchers from neighbouring Serbia [4, 5], Bulgaria [6, 7, 8] and Albania [9].

Subject of this paper is the mineralogy of vertisol in central Macedonia (Stip and Probistip). The method which is used in laboratory work for mineralogy research is roentgen difractometric method.

[II] MATERIALS AND METHODS

The Three sites were selected to present vertisols occurring in different parent materials of the study area: profile N° 2 – on clay sediment (Stip - 41°49'06.42" N, 22°11'59.71" E); profile N° 6 – on andesite tuff (Probistip - 41°54'20.74" N, 22° 09'47.95" E); and profile N° 8 – on andesite breccia (Probistip - 41°53'34.76" N, 22°11'05.64" E). Thirteen soil samples were collected from the Ap (cultivated layer of humus-accumulative horizon), A (non-cultivated layer of humus-accumulative horizon), AC (intermediate horizon) and C (parent material) horizons of pedons for laboratory analysis.

All soil samples were crushed and separated. From the individual samples were taken bigger particles and examined under binoculars. Semiquantitative analyses were performed on all soil samples. The proportions of minerals in the samples are calculated under the ratio of reflections' intensity with the greatest intensity.

The samples were shot by Difraktometar type PHILIPS PW 1051 in the area 2θ = 50 ÷ 600 for determination of the mineralogy composition without making clay analysis ("general difraktograms"). Copper radiation with a wavelength of λ CuKα = 1.54178 Á was used. The voltage on anticathode of generator "NORELCO" was 40 kV, and electric current 30 mA. The counter was moving at a speed of 2θ = 20/min. For determination of clay minerals from each sample were made two preparations in which one was shot as untreated, then saturated with glycerine and the other was burning at a temperature of 480 ^{0}C to determine the type of clay minerals in the area 2θ = 3^0 ÷ 14^0 . This means that each sample is recorded four times (once in the entire region 2θ = 5^0 ÷ 60^0) and three times: untreated - N, saturated with glycerine - G and burning at 480 ^{0}C - Z [9, 10, 11, 12]. For identification of minerals JCPDS (ASTM) file was used. Very weak reflections were not taken into accounts which are insignificant for the identification of minerals or reflections that could not be identified on this ways.

THE IIOAB JOURNAL
ISSN: 0976-3104

[III] RESULTS AND DISCUSSION

Hor. Ap (0-23cm): The sample contains quartz (Q - 72.60%), feldspates (F - 15.40%), clay minerals - montmorillonite (M - 6.80%). Calcite (C) is present with 5.20% and reflections that indicate that the zeolite is present in very small quantities are noticed **[Figure–1].**

.

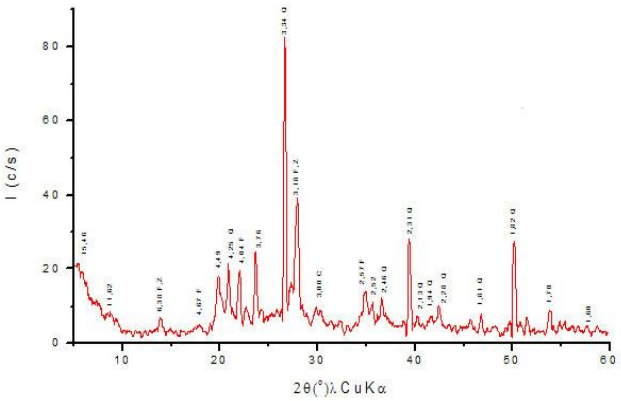

Fig. 1: Profile 2 - Ap (0-23cm)

Hor. A (23-75cm): This sample also contains quartz at most (Q - 60.51%), then clay MLM minerals (M - 13.75%), feldspates (F) and calcite (C) 10.70%, and ilite-mica are present with 5.50% **[Figure–2].**

.

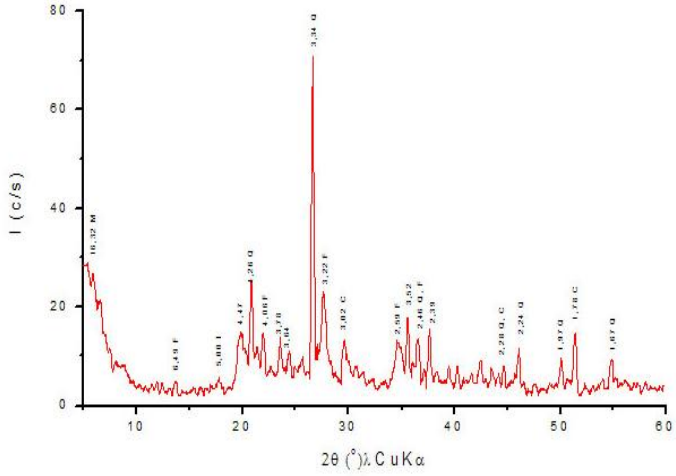

Fig. 2: Profile 2 - A (23-75cm)

Hor. AC (75-100cm): Quartz is the most present - 51.82%, montmorilonite - 18.77 and ilite (I) in very small percentage, feldspate - 16.85, and calcite - 12.1% **[Figure–3]**.

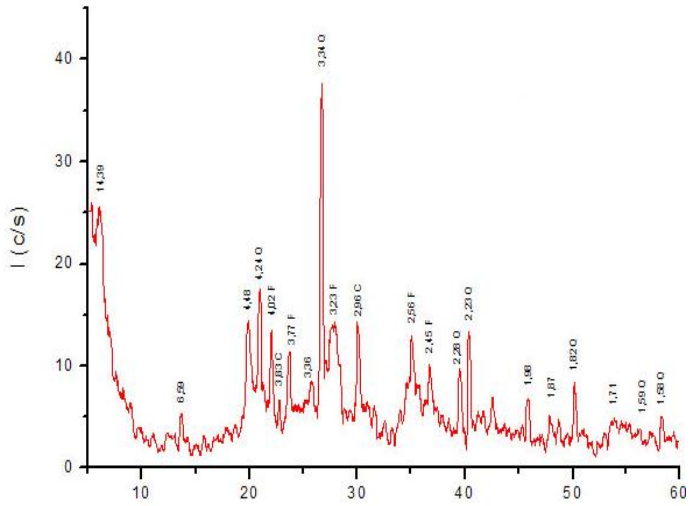

Fig. 3: Profile 2 - AC (75-100cm)

Hor. C (100-120 cm): Parent material differentiates from the other above mentioned horizons in a way that the reflections from calcite (C – 32.00%) and quartz (Q - 36.00%) have almost equal intensity. Feldspate reflections are 13.70%, clay minerals - 12.60% and the minerals from ilite-mica group - 5.30%. As for the clay minerals, they are very mixture-layered types in which montmorilonite layers participate and there is a negligible quantity of chlorite **[Figure–4]**.

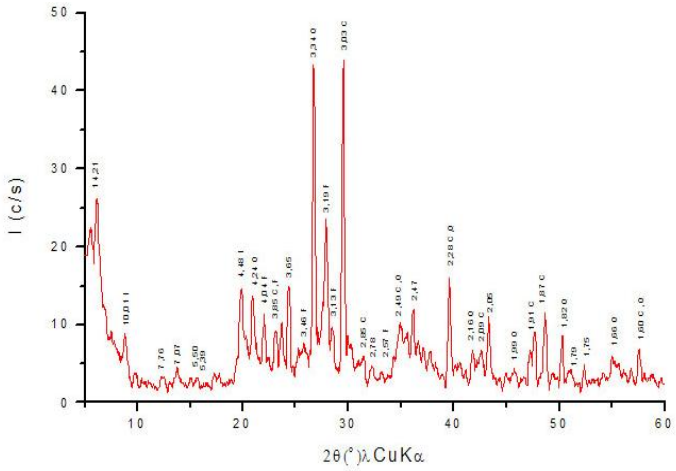

Fig. 4: Profile 2 – C (100-120cm)

Hor. Ap (0-18 cm): As before, in this sample the most present is quartz (Q - 61.10%), then feldspate (F - 26.00%), calcite (C - 6.10%), clay minerals (M - 3.50%) are mixture-layered with layers of montmorrilonite mixed with ilite-mica layers even though there are free ilite-mica minerals ((I, L) - 3.30 %). Reflections of hlorite in very small quantities are noticed **[Figure–5]**.

THE IIOAB JOURNAL
ISSN: 0976-3104

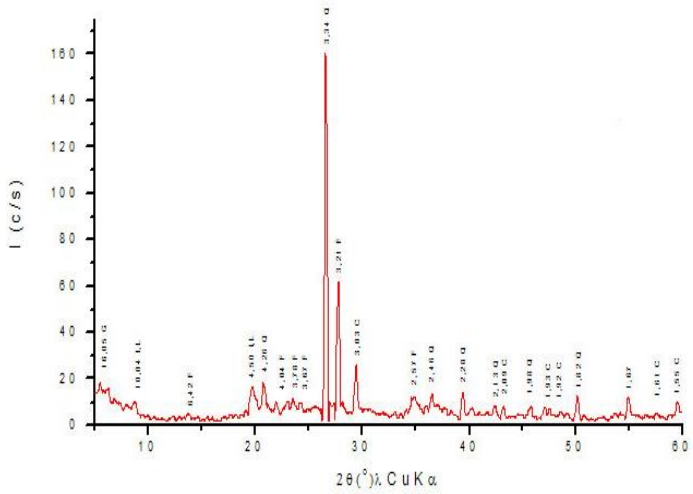

Fig. 5: Profile 6 - Ap (0-18cm)

Hor. A (21-73 cm): The sample contains mostly quartz (Q – 62.40%). Calcite is present with 18.40% and feldspate is present with 8.00%. Clay minerals are consisting mainly of mixed-layers of montmorillonite, ilitte and chlorite are present with 6.70%, while free mica-ilite minerals are present by 4.50% **[Figure–6]**.

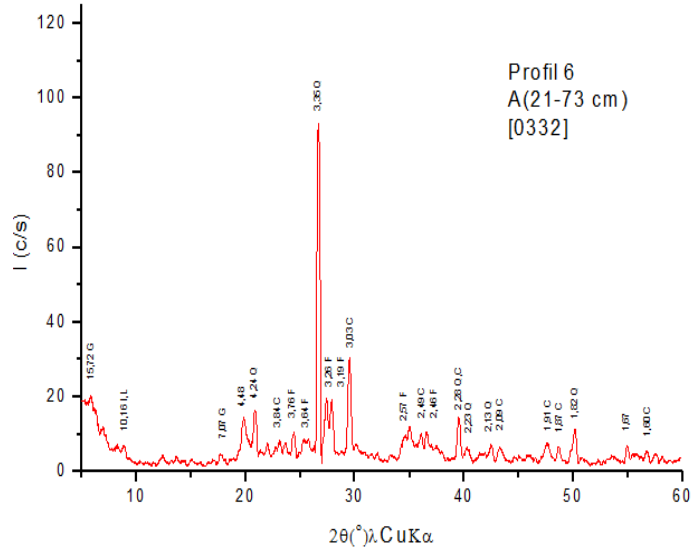

Fig. 6: Profile 6 – A (21-73cm)

Hor. AC (73-107cm): Dominant mineral is quartz with 67.80%. Calcite is presented with 23.00%. Clay minerals are presented with 4.80% (mainly ilite-montmorillonite). Free ilite-mica minerals are present by 4.00%. The presence of chlorite in very small amounts is also noticed **[Figure–7]**.

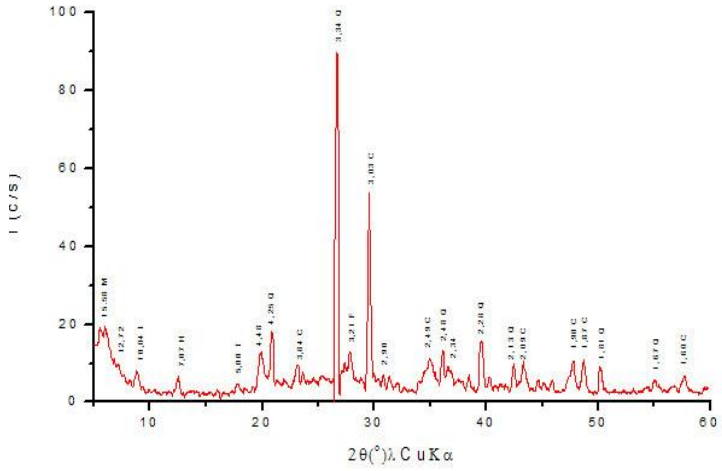

Fig. 7: Profile 6 AC (73-107cm)

Hor. C (107-130cm): this sample contains mostly quartz (Q - 46.20%), calcite (C -28.10%), than mixture-layered silicates (montmorillonite-chlorite) with 8.20%. Feldspate, dolomite and ilite-mica are present with 5.80% **[Figure–8]**.

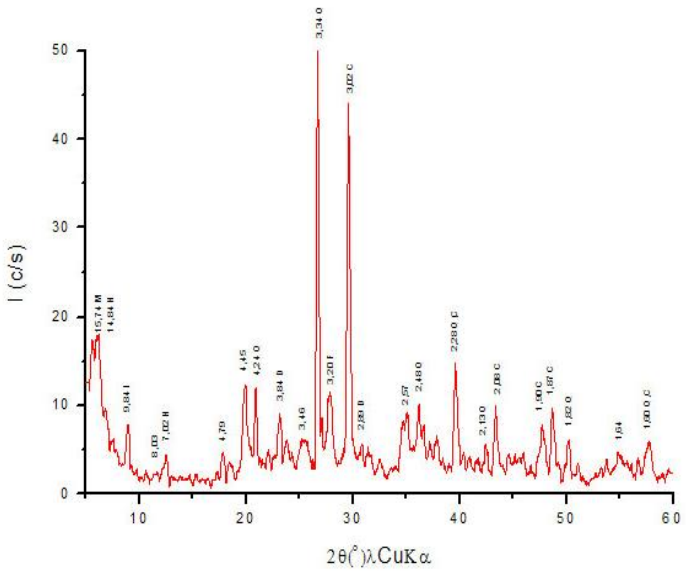

Fig. 8: Profile 6 - C (107-130)

Hor. Ap (0-26cm): Feldspate is mostly present (F-56.10%) and then quartz (Q -36.40%). Clay minerals are present with 7.4%. Ilite and calcite are present in small amounts **[Figure–9]**.

THE IIOAB JOURNAL
ISSN: 0976-3104

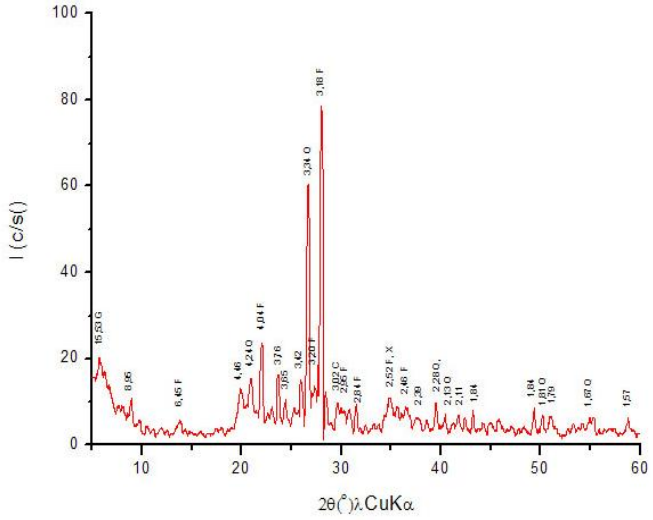

Fig. 9: Profile 8 - Ap (0-26 cm)

Hor. A (26-54 cm): in this sample dominant mineral is quartz with 75.10%, then feldspate (F - 11, 6%). Clay minerals are present with 5.30% (ilite-montmorilonite and ilite-chlorite). Calcite has approximately the same 5.30%, while free ilite is present with an insignificant quantity **[Figure−10]**.

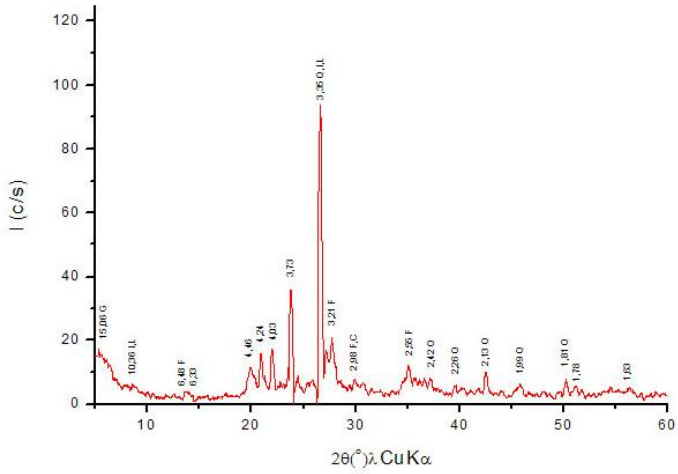

Fig. 10: Profile 8 - A (26-54 cm)

Hor. Aca (54-105 cm): The most common mineral in this sample is very unusual. Attempts by the program "MPDS" indicated a very rare mineral Koashvite Na_6 (CaMn)(Ti,Fe)SI6O18 which is registered in the records JCPDS (ASTM) under N°. 27-669. By reflection intensity of 2.52 Å, this mineral (K) is present around 81% and then quartz 12.30%. Feldspate are mostly from albeit type with 4.7%, clay minerals is present with 2.0% and they are consisted of swelling components. Reflections of free ilite are also noticed **[Figure−11]**.

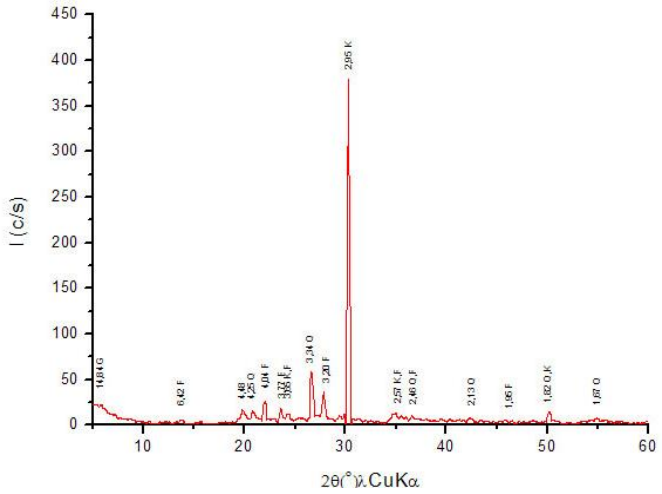

Fig. 11: profile 8 - Aca (54-105 cm)

Hor. AC (105-140 cm): the most common mineral is quartz (Q - 48.50%), than feldspate (F – 17.00%). Significant is the presence of cordierite (17.00%). Clay minerals are present with 7.50% and these are mainly mixed-layered minerals ilite-montmorillonite (ilite-chlorite) and pure chlorite. Minerals from ilite-mica group are present with 4.00% **[Figure−12]**.

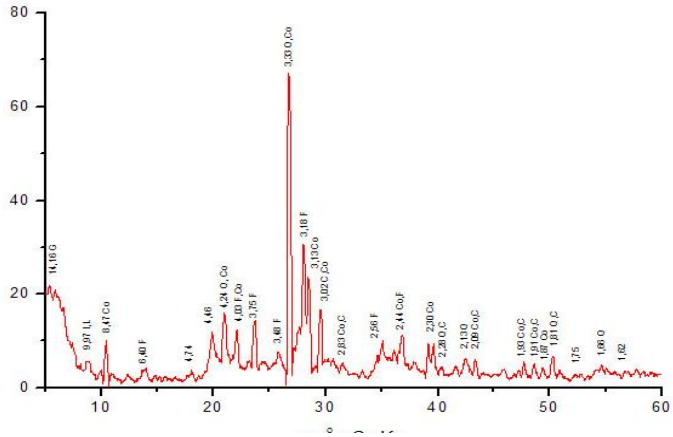

Fig. 12: Profile 8 - AC (105-140 cm)

Hor. C (140-155 cm): in this sample the most present mineral was difficult to determine. According to the literature review, by using the program "MPDS and JCPDS (ASTM) files, reflections correspond to a very rare mineral winchite (W) $NaCa(Mg,Fe,Mn,Al)_5Si_8O_{22}(OH)_2$, which according to the intensity of main reflection is represented by 45.6%, and is classified like monoclinic amphibole. Beside that this sample has feldspate (F - 23.60%,) quartz (Q - 16.4%), calcite (C - 8.90%) and clay minerals – 5.6 %. Among clay minerals prevails montmorilonite, then mixed layers ilite-montmorilonite and montmorilonite-chlorite. Minimal amounts of mica and ilite are noticed **[Figure−13]**.

THE IIOAB JOURNAL
ISSN: 0976-3104

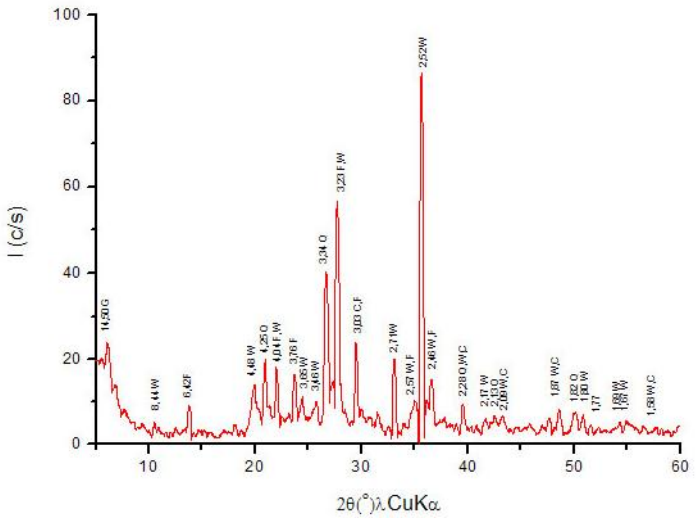

Fig. 13: Profile 8 - C (140-155 cm)

[IV] CONCLUSION

Results of the laboratory research show that quartz and feldspates are mainly present in sand and silt fractions in mineralogy of researched vertisols. According to the studied vertisols the mineralogy is inherited from the parent material and it does not significantly altered with pedogenesis. Primary and secondary minerals in parent material are created by decomposition of different rocks (mainly basic) that are found above the lake basins. The exception is profile 6 (andesite brecca) where in some horizons a very rare minerals with high percentage can be met (koashvite, winchite), which show high resistance to the chemical decomposition. Unlike the bigger fractions, monmorrilonite and mixed-layer minerals (ilite-monmorrilonite) dominate in the clay fraction and there are smaller quanities of ilite and chlorite.

The preliminary results of this study confirm the further characteristics of these rare minerals, using other methods such as scanning electron microscopy, SEM, ICP-MS and so on.
%.

FINANCIAL DISCLOSURE
This work in not supported by any grant

CONFLICT OF INTERESTS
The authors declare no conflict of Interests

REFERENCES

[1] Filipovski GJ. [1966] Soils of the Republic of Macedonia, Vol. II. Macedonian Academy of Science and Arts, Skopje. JCPDS kartoteka (ASTM).
[2] Мюкенхаузен Е. [1967] Електроната микроскопия в помош на почвено-генетическите изследования, Почвознание и агрохимия, т. 2, No. 3, София.
[3] Dudal R. [1965] Dark clay soils of tropical and subtropical regions. FAO Agricultural Development Paper No. 83. FAO, Rome, Italy, 161pp.
[4] Brown G. [1961] The X-ray identification and crystal structures of clay minerals. Min. Soc. London.
[5] Thorez, J. [1976] Practical identification of clay minerals. Ed. G. Lellote B4820 Dison Belgique.
[6] Антипов-Каратаев НИ, Танов Е, Галева В, Демянов К, Палавеев Т, et al. [1960] Черноземи смолници. Почвите в България, Земиздат, София.
[7] Lippman F. [1968] *Contr. Mineral & petrol* 19 pp.: 260–270.
[8] Nejgebauer V, Zakosek H. [1962] Die smonitza, Notizbl. Hess. Bodenforsch, No 90, Wiesenbanden.
[9] Manuševa L. [1961] Karakter koloida u smonicama Makedonije, Arhiv za poljoprivredne nauke, god. XIV. S. 43, Beograd.
[10] Ђурић С. [1999] Одређивање глиновитих минерала рендгенском дифракцијом. Издања 99. 53 (1997), 7, 8, 9, Београд, стр. 224–227.
[11] Ђурић С. [2002] Методе истраживања у кристалографији. Техн. Фак. Чачак. ИТН. САНУ. Београд, стр. 207–213.
[12] Živković M, Pantović M, Aleksandrović D. [1964] O smonicama Aleksinačke kotline, Zemlj. I biljaka, Vol. 13, No. 3, Beograd.